

1

2 **Robust lysosomal rewiring in Mtb infected macrophages mediated** 3 **by Mtb lipids restricts the intracellular bacterial survival**

4 Kuldeep Sachdeva¹, Manisha Goel¹, Malvika Sudhakar^{2,3}, Mansi Mehta⁴,
5 Rajmani Raju⁴, Karthik Raman^{2,3}, Amit Singh⁴, Varadharajan
6 Sundaramurthy^{1*}

7 1. National Center for Biological Sciences, Tata Institute of Fundamental Research,
8 Bengaluru, 560065, India

9 2. Department of Biotechnology, Indian Institute of Technology Madras, Chennai, 600
10 036, India

11 3. Initiative for Biological Systems Engineering, Robert Bosch Centre for Data Science
12 and Artificial Intelligence (RBC-DSAI), Indian Institute of Technology Madras, Chennai, 600
13 036, India

14 4. Center for Infectious Disease Research, Department of Microbiology and Cell Biology,
15 Indian Institute of Science, Bengaluru, 560 012, India

16 * Correspondence: varadha@ncbs.res.in

17 **Abstract**

18 Intracellular pathogens commonly manipulate the host lysosomal system for their survival,
19 however whether this affects the organization and functioning of the endo-lysosomal system
20 itself is not known. Here, we show using *in vitro* and *in vivo* infections that the lysosomal
21 content and activity is globally elevated in *M. tuberculosis* infected macrophages. The
22 enhanced lysosomal state is sustained over time and defines an adaptive homeostasis of the
23 infected cell. Lysosomal alterations are caused by mycobacterial surface components,
24 notably the cell wall lipid SL-1, which functions through the mTORC1-TFEB axis. Mtb mutant
25 defective for SL-1 levels shows reduced lysosomal content and activity compared to wild
26 type. Importantly, this phenotype is conserved during *in vivo* infection, as well as in clinical
27 Mtb isolates that are deficient in SL-1. The alteration in lysosomal phenotype in mutant Mtb
28 lead to decreased lysosomal delivery of Mtb, and importantly, increased survival of
29 intracellular Mtb. These results define the global alterations in the host lysosomal system as
30 a crucial distinguishing feature of Mtb infected macrophages that is host protective and
31 contribute to the containment of the pathogen.

32

33 **Keywords:** tuberculosis, endocytosis, lysosomes, homeostasis, Sulfolipid SL-1,
34 heterogeneity, endocytic capacity, host-pathogen interaction, adaptive lysosomal
35 homeostasis, TFEB

36

37

1 INTRODUCTION

2 *M. tuberculosis* is considered as one of the most successful infectious agents known to
3 mankind. A large part of this success is due to the ability of the bacteria to manipulate and
4 interfere with the host system at multiple levels. At a cellular level, in order to establish and
5 sustain the infected state, *M. tuberculosis* significantly interferes with the host cell trafficking
6 pathways, such as phagosome maturation (Armstrong and Hart, 1971; Cambier et al., 2014;
7 Pieters, 2008; Russell, 2001) and autophagy (Gutierrez et al., 2004; Kumar et al., 2010). In
8 cultured macrophages *in vitro*, *M. tuberculosis* prevents the fusion of phagosomes to
9 lysosomes, instead residing in a modified phagosome (Armstrong and Hart, 1971; Russell,
10 2001). During *in vivo* infections, *mycobacteria* are delivered to lysosomes (Levitte et al.,
11 2016; Sundaramurthy et al., 2017) after an initial period of avoiding it (Sundaramurthy et
12 al., 2017). Despite encountering acidic conditions in lysosomes *in vivo*, *mycobacteria*
13 continue to survive (Levitte et al., 2016; Sundaramurthy et al., 2017), showing that
14 additional acid tolerance mechanism is involved (Levitte et al., 2016; Vandal et al., 2008).
15 Encounter with the host cell lysosomal pathway, in both avoiding it and adapting to it, is
16 critical for the intracellular life of mycobacteria.

17 Despite the bacteria itself residing in an arrested phagosome *in vitro*, *M. tuberculosis*
18 infection could impact the endo-lysosomal system globally, since mycobacterial surface
19 components, including distinct lipids, accumulate in late endosomes and lysosomes, (Beatty
20 et al., 2001; Beatty et al., 2000; Beatty and Russell, 2000; Russell et al., 2002). Infact,
21 individual mycobacterial lipids modulate vesicular trafficking in the host cells. For example,
22 Phosphatidylinositol Mannoside (PIM) specifically increases the homotypic fusion of
23 endosomes and also endosome-phagosome fusion (Vergne et al., 2004), Lipoarabinomannan
24 (LAM) inhibits the trafficking of hydrolases from Trans-Golgi-Network (TGN) to late
25 phagosome-lysosome and also inhibits the fusion of late endosomes to late phagosomes
26 (Fratti et al., 2003), Trehalose dimycolate decreases late endosome-lysosome fusion and
27 lysosomal Ca²⁺ release (Fineran et al., 2017). These interactions suggest significant
28 interferences with the endo-lysosomal network during *M. tuberculosis* infection. Indeed,
29 increased lysosomal content is reported in *M. tuberculosis* infected mouse tissues *in vivo*
30 (Sundaramurthy et al., 2017). However, only a few studies have systematically addressed
31 such global alterations. Podinovskaia et al showed that the trafficking of an independent
32 phagocytic cargo is significantly altered in *M. tuberculosis* infected cell (Podinovskaia et al.,
33 2013), arguing that *M. tuberculosis* infection globally affects phagocytosis.

34 Phagosome maturation from a nascent phagosome to phagolysosome requires sequential
35 fusion with early endosomes, late endosomes and lysosomes (Desjardins, 1994; Fairn and
36 Grinstein, 2012; Levin et al., 2017), hence optimal endosomal trafficking is necessary for
37 phagosomal maturation. Consequently, pharmacological activation of endosomal trafficking
38 overcomes *mycobacteria* mediated phagosome maturation arrest, and negatively impacts
39 intracellular mycobacterial survival (Sundaramurthy et al., 2017). Similarly,
40 pharmacological and physiological modulation of autophagy results in delivering
41 *mycobacteria* to lysosomes (Deretic, 2014; Gutierrez et al., 2004; Ponpuak et al., 2010;
42 Sundaramurthy et al., 2013) and increasing the total cellular lysosomal content
43 (Sundaramurthy et al., 2013). Mycobacterial survival within macrophages could thus be
44 sensitive to alterations in the host endo-lysosomal system.

1 Phagocytosis and lysosomes are coupled by signaling pathways, where phagocytosis
2 enhances lysosomal bactericidal properties (Gray et al., 2016) and concomitant lysosomal
3 degradation is important for sustained phagocytosis at the plasma membrane (Wong et al.,
4 2017). Hence lysosomal homeostasis plays a crucial role during infections. The traditional
5 view of lysosomes as the ‘garbage bin’ of the cell is undergoing dramatic revisions in recent
6 years, with lysosomes emerging as a signaling hub integrating diverse environmental,
7 nutritional and metabolic cues to alter cellular response (Lim and Zoncu, 2016; Settembre et
8 al., 2013). Importantly, lysosomal biogenesis itself is one such major downstream response,
9 which is orchestrated by transcription factors of the microphthalmia family, notably TFEB
10 (Bouché et al., 2016; Ploper and De Robertis, 2015; Ploper et al., 2015; Yang et al., 2018).
11 Whether or not *M. tuberculosis* or its components impacts these processes is not known.

12 In this study, we focus on the global alterations in the macrophage lysosomal system and
13 show that it is significantly increased in *M. tuberculosis* infected macrophages compared to
14 non-infected cells. This increase is robust and defines an altered homeostatic state in the
15 infected cells. Modulations in the lysosomal system are mediated by diverse mycobacterial
16 surface components, such as the Sulfolipid SL-1 and PIM6. Purified SL-1 induces lysosomal
17 biogenesis in an mTORC1-TFEB dependent manner, while an *M. tuberculosis* mutant strain
18 lacking SL-1 shows correspondingly reduced altered lysosomal homeostasis both *in vitro*
19 and *in vivo*. The attenuated lysosomal rewiring in SL-1 mutant results in reduced trafficking
20 to lysosomes and an enhanced intracellular survival of the mutant bacteria.

21 **Material and methods**

22 **Mycobacterial strains and growth conditions**

23 *Mycobacterium tuberculosis* (H37Rv) expressing GFP was provided by Dr. Amit Singh (Indian
24 Institute of Science, Bangalore). *Mycobacterium bovis* BCG expressing GFP was a kind gift
25 from Jean Pieters (University of Basel). Wild type *M. tuberculosis*, Strain CDC1551, (NR-
26 13649) and *M. tuberculosis* Δ *pks2*, Strain CDC1551: Transposon Mutant 1046 (MT3933,
27 Rv3825c, NR-17974) were obtained from BEI resources, NIAID, NIH. Wild type and Δ *pks2*
28 CDC1551 *M. tuberculosis* strains were transformed with pMV762-roGFP2 vector (a kind gift
29 from Dr. Amit Singh, IISc, Bangalore) for subsequent experiments. Mycobacterial strains
30 were grown in Middlebrook 7H9 (BD Difco 271310) supplemented with 10% of OADC (BD
31 Difco 211886) at 37°C. Before infection bacterial clumps were removed by centrifugation at
32 80g and supernatant was pelleted, re-suspended in RPMI media and used for infection.
33

34 **Cell culture and infection**

35 THP1 monocytes were cultured in RPMI 1640 (Gibco™ 31800022) supplemented with 10%
36 fetal bovine serum (Gibco™ 16000-044). THP1 monocytes were differentiated to
37 macrophages by treatment with 20 ng/ml phorbol myristate acetate (PMA) (Sigma-Aldrich
38 P8139) for 20 hours followed by incubation in PMA free RPMI 1640 media for two days and
39 used for infections. Differentiated THP1 macrophages were incubated with *mycobacteria* for
40 4 hours followed by removal of extracellular bacteria by multiples washes. Infected cells
41 were fixed with 4% paraformaldehyde (Sigma 158127) at 2 and 48 hours post infection
42 (hpi) and were used for subsequent experiments. For infection in RAW macrophages,
43 bacteria were incubated with cells for 2hrs followed by removal of extracellular bacteria by

1 multiples washes. Human primary monocyte were isolated from buffy coats and
2 differentiated to macrophages as described previously (Sundaramurthy et al., 2014;
3 Sundaramurthy et al., 2013) and used for infection assays.

4

5 **CFU assay**

6 THP1 monocyte derived macrophages were infected with wild type or *pks2* KO CDC1551 *M.*
7 *tuberculosis*-GFP. At 0hr and 48hrs post infection, cells were lysed with 0.05% SDS (Himedia
8 GRM205) and plated in multiple dilutions on 7H11 (BD Difco 0344C41) agar plates. Colonies
9 were counted after incubation at 37°C for 3-4 weeks.

10

11 **Immuno-staining, imaging and image analysis**

12 For immunostaining of different markers, differentiated THP1 macrophages after infection
13 were fixed with 4% paraformaldehyde, washed with PBS and permeabilized with SAP buffer
14 [0.2% Saponin (Sigma-Aldrich S4521), 0.2% Gelatin (Himedia Laboratories TC041) in PBS]
15 for 10 min at room temperature. Primary antibodies Lamp1 (DSHB H4A3) and Lamp2
16 (DSHB H4B4), Anti-Mtb (Genetex GTX20905) were prepared in SG-PBS (0.02% Saponin,
17 0.2% Gelatin in PBS) and incubated overnight at 4°C. Gelatin in the buffers was used as a
18 blocking agent and saponin as detergent. After washing with SG-PBS, cells were incubated in
19 Alexa tagged secondary antibodies (Life Technologies, Invitrogen) prepared in SG-PBS for
20 1hr at room temperature, washed, stained with 1µg/ml DAPI and 3µg/ml Cell Mask Blue
21 (Life Technologies, Invitrogen), and imaged using either confocal microscopes FV3000, the
22 automated spinning disk confocal Opera Phenix (Perkin Elmer) or Nikon Ti2E.

23 Images were analysed by either CellProfiler, Harmony or Motiontracking image analysis
24 platforms. CellProfiler pipelines similar to previously established ones (Sundaramurthy et
25 al., 2014; Sundaramurthy et al., 2017) were used. In all cases, images were segmented to
26 identify nuclei, cells, bacteria and lysosomal compartments. Objects such as bacteria and
27 endo-lysosomes were related to individual cells to obtain single cell statistics, and multiple
28 parameters relating to their numbers, sizes, intensities as well as intra-object associations
29 were extracted. MS excel and RStudio platform with libraries ggplot2, dplyr and maggitr was
30 used for data analysis and plotting. Most data are plotted as box plots which show the
31 minimum, 1st quartile, median, 3rd quartile and maximum values. Individual data points
32 corresponding to single cells are overlaid on the boxplots. Statistical significance between
33 different sets was determined using Mann-Whitney unpaired test or unpaired Student's T-
34 test with unequal variance.

35 **Flow cytometry**

36 Samples were analyzed using FACS Aria Fusion cytometer. Using FSC-Area vs SSC-Area
37 scatter plot, macrophage population was gated for further use. Based upon fluorescence
38 level in the uninfected sample, gates for uninfected and infected cells were defined. Further,
39 cargo uptake, endosomal and lysosomal levels were compared between the gated infected
40 and uninfected populations. For each sample, 10,000 gated events were acquired. FSC files
41 exported using FlowJo were subsequently analyzed by RStudio.

42

43 **Identifying important morphological features from High content image analysis and** 44 **classification of infected cells from lysosomal features**

1 Two separate datasets from human primary macrophages infected with *M. bovis* BCG-GFP
2 (named Exp1 and Exp2) were used for analysis. Dataset Exp1 contained a total of 37,923
3 cells out of which 18,546 were infected. Dataset Exp2 contained a total of 36,476 cells out of
4 which 15,022 were infected. Each dataset has multiple features relating to cells, bacteria and
5 lysosomes, as well as their associations with each other. Out of these features, 16 lysosomal
6 parameters and 11 cellular parameters were chosen for further analysis. The data was split
7 into training and test set (7:3) and the model was trained using logistic regression with an
8 L1 penalty. Logistic regression uses a logistic function to model one or more independent
9 variables in order to predict a categorical variable (Pedregosa et al., 2011).
10 Applying an L1- regularization penalty using the parameter c forces the weights of many of
11 the features to go to zero. The best regularization parameter was identified by 20-fold cross-
12 validation on the training set. Since all the features were selected for the best regularization
13 parameter ($c = 1$), we further reduced c . Classification metrics, accuracy, precision, recall
14 and F1 score were calculated for infected and non-infected cells for a range of regularization
15 parameters (1, 0.1, 0.01, 0.001, 0.0005, 0.0001 and 0.00018). The value of $c = 0.00018$
16 forces the model to pick a single feature for classification. Accuracy is defined as total true
17 predictions divided by false predictions. Precision measures the ability of the model to make
18 correct predictions. Recall measures the fraction of correct predictions from the total
19 number of cells belonging to the given class. F1-score is the harmonic mean of precision and
20 recall. F1-score, precision and recall were calculated for each class (infected, non-infected).
21 To find the contribution of individual feature for classification accuracy, we used logistic
22 regression on single features with 20-fold cross-validation and reported the accuracy of
23 training and test set for both datasets.

24 The random forest algorithm considers predictions of multiple decision trees to perform
25 classification (Breiman, 2001; Pedregosa et al., 2011). Further, a random forest also enables
26 us to rank the features, by measuring the contribution of individual features to each of the
27 constituent decision trees. Note that random forests thus use multiple models, in contrast to
28 logistic regression, which builds a single model; in both cases, the goal is to classify a cell as
29 infected or non-infected. Parameters for random forest were estimated using grid search
30 with 20-fold cross-validation. The best parameters were based on maximum average
31 accuracy and were used for finding feature contribution and ranking.

32 For infections in THP-1 monocyte derived macrophages (with *M. bovis* BCG-GFP, or *E. coli*),
33 similar analysis was done, with a difference that the features were extracted from the
34 images using Harmony image analysis platform.

35 **Cargo pulsing and Functional endocytic assays**

36 Alexa labeled Human Holo-Transferrin (Life Technologies, Invitrogen T23365, T2336;
37 5 μ g/ml) and Dextran (Life Technologies, Invitrogen D22914, D-1817; 200 μ g/ml) were used
38 to quantify endocytic uptake capacity in cells. Cargo pulse for endocytic assays was
39 performed by individually diluting the respective cargo at indicated concentrations in RPMI
40 media and incubated with cells at 37°C and 5% CO₂, followed by washing with media and
41 fixing with 4% paraformaldehyde. LysoTracker Red (Life Technologies, Invitrogen L7528;
42 100nM) and Magic red cathepsin B (MRC) (Bio-Rad ICT937) were used to stain lysosomes in
43 the cells. For lysoTracker red labeling, cells were incubated in complete RPMI containing

1 100nM lysotracker red for 30 min and 1hr for MRC followed by fixation with 1%
2 paraformaldehyde for 1 hour at room temperature.

3

4 ***In vivo* infection and single cell suspension preparation**

5 BALB/c or C57BL/6J or C57BL/6NJ mice were infected with *M. tuberculosis* GFP using Glas-
6 Col inhalation exposure chamber (at the indicated CFU). Mice were sacrificed post-infection
7 at the indicated timepoints, and infected lungs were dissected out, minced and placed in
8 Miltenyi GentleMACS C-tubes containing 2ml dissociation buffer (RPMI media with
9 0.2mg/ml Liberase (Sigma Aldrich 5466202001) and 0.5mg/ml DNAase (Sigma Aldrich
10 11284932) and subjected to the inbuilt lung dissociation protocol 1 of Miltenyi GentleMACS,
11 followed by incubation at 37°C and 5% CO₂ for 30 min with low agitation (50 rpm) and a
12 second 20-second dissociation with lung dissociation protocol 2 (Miltenyi GentleMACS). The
13 suspension was passed through 70-micron cell strainer and then pelleted at 1200 rpm for 5
14 min. Pellet was re-suspended in 1ml erythrocyte lysis buffer (155 mM NH₄Cl, 12 mM
15 NaHCO₃ and 0.1 mM EDTA) for 1 min and immediately added to 10 ml RPMI media. Cells
16 were centrifuged again, re-suspended in RPMI media with 10% fetal bovine serum, and
17 plated for 2 hours in RPMI media with 10% fetal bovine serum for macrophage selection
18 based on adherence. After 2 hours, non-adhered cells were washed and adhered cells were
19 used for the assay. Adherent cells were immunostained with F4/80 PE-Vio615 (Miltenyi
20 Biotec REA126) and CD11b (DSHB M1/70.15.11.5.2) antibody to check for macrophage
21 purity.

22

23 ***M. tuberculosis* component screen**

24 The following *M. tuberculosis* surface components were obtained through BEI resources,
25 NIAID, NIH: *Mycobacterium tuberculosis*, Strain H37Rv, Purified Phosphatidylinositol
26 Mannosides 1 & 2 (PIM_{1,2}), NR-14846; *Mycobacterium tuberculosis*, Strain H37Rv, Purified
27 Phosphatidylinositol Mannoside 6 (PIM₆), NR-14847; *Mycobacterium tuberculosis*, Strain
28 H37Rv, Purified Lipoarabinomannan (LAM), NR-14848; *Mycobacterium tuberculosis*, Strain
29 H37Rv, Purified Lipomannan (LM), NR-14850; *Mycobacterium tuberculosis*, Strain H37Rv,
30 Total Lipids, NR-14837; *Mycobacterium tuberculosis*, Strain H37Rv, Purified Trehalose
31 Dimycolate (TDM), NR-14844; *Mycobacterium tuberculosis*, Strain H37Rv, Purified
32 Sulfolipid-1 (SL-1), NR-14845; NR-14850; *Mycobacterium tuberculosis*, Strain H37Rv,
33 Purified Mycolylarabinogalactan-Petidoglycan (mAGP), NR-14851; *Mycobacterium*
34 *tuberculosis*, Strain H37Rv, Purified Arabinogalactan, NR-14852; *Mycobacterium*
35 *tuberculosis*, Strain H37Rv, Purified Mycolic Acid Methyl Esters, NR-14854; *Mycobacterium*
36 *tuberculosis*, Strain H37Rv, Mycobactin (MBT), NR-44101; *Mycobacterium tuberculosis*,
37 Strain H37Rv, Purified Trehalose Monomycolate (TMM), NR-48784. They were
38 reconstituted according to the supplier's instruction and treated on differentiated THP1
39 cells at the indicated concentration. Components that affected lysosomes were selected for
40 further use.

41

42 **Immunoblotting**

43 To compare protein levels by immunoblotting, PMA differentiated THP1 cells were treated
44 with selected mycobacterial surface components, lysed using cell lysis buffer (150mM Tris-

1 HCL, 50mM EDTA, 100mM NaCl, Protease inhibitor cocktail) at 4°C for 20 min, passaged
2 through 40-gauge syringe followed by centrifugation at 14000 rpm for 15 min at 4°C and the
3 supernatant was used for blotting. The following antibodies were used: p70 S6 kinase
4 (49D7), phospho-p70 S6 kinase (Thr389), phosphor-4E-BP1 (2855T), 4E-BP1 (9644T),
5 GAPDH (5174S) and β actin (13E5). These antibodies were procured from Cell Signaling
6 Technologies. LAMP-1 (H4A3 and 1D4B) antibodies were procured from DSHB
7 [Developmental Studies Hybridoma Bank].

8

9 **Cell transfection and Nuclear-cytoplasmic TFEB translocation**

10 pEGFP-N1-TFEB was a gift from Shawn Ferguson (Addgene plasmid # 38119). HeLa cells
11 were seeded at 70% confluency in 8 well chambers and transfected with lipofectamine 2000
12 (ThermoFisher Scientific, 11668030). For RAW macrophages, lipofectamine 3000
13 (ThermoFisher Scientific, L3000015) was used. Transfection was performed following
14 manufacturer's protocol. Transfection complex was washed after 6 hours, and SL-1
15 treatment was started 12 hours post-transfection. Cells were fixed and imaged after 24
16 hours of SL-1 treatment (25 μ g/ml). The boundary of transfected cells was marked manually
17 based on bright field or cytoplasmic stain- cell mask blue and DAPI signal was used to
18 segment nucleus. Nuclear-cytoplasmic translocation of TFEB was assessed by comparing
19 TFEB fluorescence ratio between nuclear and cytoplasmic regions. For siRNA transfection,
20 15,000 THP1 cells were seeded per well in 384 well plate and were transfected with either
21 universal negative control 1 (UNC1) (Millipore Sigma, SIC001) or esiRNA human TFEB
22 (Millipore Sigma, EHU059261) siRNA using lipofectamine RNAimax (Thermo Fisher
23 Scientific, 13778100) according to manufacturer's protocol for 48hrs and was used for
24 further experiments.

25

26 **RESULTS**

27 ***M. tuberculosis* infected macrophages have elevated lysosomal content than** 28 **uninfected bystander cells**

29 To assess the if there are changes in the total lysosomal content during mycobacterial
30 infections, we infected human primary monocyte derived macrophages with *M. bovis* BCG,
31 stained with acidic probe lysotracker red, fixed the cells 48 hours post infection and imaged.
32 Images were segmented using the methods described earlier (Sundaramurthy et al., 2014;
33 Sundaramurthy et al., 2013; Sundaramurthy et al., 2017), to extract number, intensity and
34 morphology-related features of bacteria and lysosomes within individual macrophages.
35 Typically, 50-60% cells were infected under these experimental conditions; hence, statistics
36 could be obtained from a reliably large number of both infected and uninfected cells from
37 the same population at a single cell resolution. First, we compared the total number and
38 total intensity of lysosomes between individual infected and uninfected cells. The results
39 show that infected cells on an average have more lysotracker positive vesicles and
40 integrated intensity than uninfected cells (Fig 1A). Similar results were obtained in THP-1
41 monocytederived macrophages infected with *M. tuberculosis* H37Rv expressing GFP (Fig 1B)
42 and stained with lysotracker red. Lysotracker red stains acidic vesicles but is not specific for
43 lysosomes. In order to further confirm the global alterations in lysosomes upon *M.*
44 *tuberculosis* infection, we repeated these experiments with two lysosome activity probes,
45 Magic Red Cathepsin (MRC) and DQ-BSA, which are cell-permeable fluorogenic dyes that

1 fluoresce when exposed to the hydrolytic lysosomal proteases. The results (Fig 1C, D) show
2 that the number and total fluorescence of both MRC and DQ-BSA positive vesicles are higher
3 in *M. tuberculosis* infected cells compared to non-infected cells suggesting that the lysosomes
4 in infected cells are functional in terms of their proteolytic activity. In order to
5 independently verify this result, we immunostained *M. bovis* BCG infected THP1
6 macrophages with antibodies against two commonly used lysosomal markers, Lamp1 (Fig
7 S1A, C) and Lamp2 (Fig S1B, D), and assessed the lysosomal content by imaging assay. In
8 both the cases, infected cells showed higher lysosomal content than uninfected cells.
9 Moreover, the elevated lysosomal content in *mycobacteria* infected cells was observed at
10 both 2 hours post infection (hpi) and 48 hpi (Fig 1B-D, S1A-D). Independently, Lamp1 levels
11 were also measured at 2, 24 and 48hrs in *M. bovis* BCG infected THP1 macrophages by flow
12 cytometry. In all the timepoints measured, infected cells showed higher lysosomal content
13 than uninfected cells (Fig S1E). Together, these results show that the enhanced lysosomal
14 content and activity are sustained over time in Mtb infected macrophages. In cultured
15 macrophages *in vitro*, it is well established that majority of the pathogenic *mycobacteria* are
16 not delivered to lysosomes but remain in an arrested phagosome. We tested the co-
17 localisation of Mtb with the different lysosomal probes quantitatively (Fig S1C). Analysis of
18 the lysosomal delivery of more than 10,000 intracellular *Mtb* using multiple lysosomal
19 probes shows that inline with earlier observations, majority of Mtb did not co-localise with
20 lysosomes (Fig 1 E-G).

21

22 **Lysosomal features alone can predict the infection status of a cell**

23 Given the reproducible alterations in lysosomes upon mycobacterial infection, we tested if
24 an infected cell can be predicted solely based on the lysosomal features, in the absence of
25 any information from bacteria. We used multiple features of the lysosomes, which report
26 diverse aspects of lysosomal biology such as the intensity, size, elongation and distribution
27 within the cell (Table 1) for this purpose. We used two separate datasets of human primary
28 monocyte derived macrophages infected with *M. bovis* BCG-GFP (Exp1 and Exp2). Dataset
29 Exp1 contained 37,923 cells out of which 18,546 were infected, while dataset Exp2
30 contained 36,476 cells out of which 15,022 were infected. The data were split into training
31 and test sets, and a model was trained using logistic regression, as described in methods.
32 The results showed that the model can indeed identify infected cells with ~90% accuracy
33 (Fig 1H). Accuracy measures the fraction of true predictions made by the model. For the
34 Exp1 dataset, accuracy varied from 0.717 to 0.821 for the test set as we increased the number of
35 features used for classification. In order to identify the individual lysosomal features
36 contributing maximally for accurate identification of infected cells, we iterate over different
37 sets of parameters. This analysis revealed that a subset of seven features showed the highest
38 contribution, with an accuracy of 0.800, showing that maximum information is captured by
39 this subset of features. Similarly, for the Exp2 dataset, the accuracy values vary between
40 0.770 to 0.849, with an accuracy of 0.841 for a subset of six features. Single feature analysis
41 showed that the top 11 features selected by both datasets are identical, showing that the
42 features selected are data independent. Further, analyses using an independent algorithm
43 (random forest) reiterated the importance of these features as they are once again ranked in
44 the top 11 and contribute >70% during classification. We obtained similar results in another
45 dataset describing THP-1 monocyte derived macrophages infected with *M. bovis* BCG-GFP.

1 The accurate prediction of an infected cell solely based on lysosomal parameters in the
2 absence of any information from the bacterial channel, and the remarkable consistency
3 across different experimental datasets and infection conditions shows the robustness of the
4 alterations in lysosomes upon mycobacterial infection.

5

6 **Lysosomal alterations *in vivo***

7 Next, we tested if similar lysosomal rewiring is observed during *in vivo* infection. We
8 infected BALB/c mice with *M. tuberculosis* expressing GFP using aerosol infection. After four
9 weeks, we prepared single cell suspensions from infected lungs and isolated macrophages.
10 The identity of these cells were tested using F4/80 and CD11b, two markers frequently used
11 to characterize murine macrophages (Zhang et al., 2008), and were found to be over 90%
12 positive (Fig S2 A-D). We stained these cells with lysotracker red, or immunostained for
13 antibodies against Lamp1 and Lamp2 followed by assessment of the total lysosomal content
14 between infected and uninfected cells. The results, compiled from 4 individual mice (Fig 2A-
15 C), show increased lysosomes specifically in infected cells. Similarly, single cell suspensions
16 from infected mice pulsed with functional lysosomal probes MRC and DQ-BSA showed
17 higher number and total cellular fluorescence of lysosomes in infected cells compared to
18 non-infected (Fig 2 D, E). Similar results were obtained with C57BL/6J mice (Fig 5G-I),
19 showing that these alterations are robust and strain independent.

20

21 While these results suggest that lysosomes are rewired *in vivo* during Mtb infection, there
22 are two potential confounding factors for this interpretation. First, the time point used for
23 these infections (4 or 6 weeks) could result in immune activation which could influence our
24 results. Second, we used high aerosol inocula. Although, both the high inocula and longer
25 infection time was necessary to obtain sufficient number of infected cells from mice for
26 robust statistical analysis, they could cause artefacts.. In order to test if these factors are
27 significantly influencing the results, we first infected THP-1 monocyte derived macrophages
28 with Mtb-GFP and treated with 25 ng/ml IFN- γ for 48 hpi followed by staining with
29 lysotracker red. Quantification of total cellular lysotracker content reveals that, while as
30 expected, there is an increase in net lysosomal content upon IFN γ treatment, Mtb infected
31 cells showed a further increase (Fig S2 E, F). These results suggest that the lysosomal
32 rewiring during Mtb infection is autonomous of immune activation status. As expected, the
33 co-localisation of Mtb with lysotracker red was also higher in IFN γ treated condition (Fig S2
34 G). Next, we infected BALB/c mice with low aerosol inocula (~150 cfu) for shorter time
35 point. We isolated infected macrophages from mice ~2 weeks post infection and stained
36 with lysotracker red or MRC. Data, pooled from multiple infected mice show (Fig S2 H, I)
37 similar alterations in lysosomes *in vivo* even at low CFU infection and shorter infection time
38 point. Thus, the rewiring of host lysosomes observed *in vitro* is also conserved during *in vivo*
39 infections.

40 While it is well known that *M. tuberculosis* and *M. bovis* BCG avoid delivery to lysosomes
41 during infections in cultured macrophages *in vitro*, recent reports have shown that *in vivo*,
42 *mycobacteria* are delivered to lysosomes and continue to survive, albeit at a reduced rate

1 (Levitte et al., 2016; Sundaramurthy et al., 2017). Hence, we checked the lysosomal delivery
2 of *M. tuberculosis* *in vivo* in macrophages isolated from infected mouse lungs from BALB/c
3 mice. The results (Fig 2 F) show that ~30-40% of Mtb are delivered to lysosomes in the time
4 point tested for the indicated lysosomal probes. Together, these results identify adaptive
5 lysosomal homeostasis as a defining aspect of *M. tuberculosis* infection in macrophages
6 during both *in vitro* and *in vivo* infections.

7 **Lysosomal profiles of macrophages infected with *mycobacteria* and *E. coli* are distinct from** 8 **each other**

9 In the assays described above, we have compared lysosomal content and activity from
10 infected and uninfected cells from the same population. Uninfected cells in the same milieu
11 as infected cells are subjected to bystander effects (Beatty et al., 2001; Beatty et al., 2000)
12 and may not be true representatives of a non-perturbed macrophage cell. Hence, we
13 compared the distributions of total cellular lysosomal content between *M. tuberculosis*-GFP
14 infected, bystander and naïve THP-1 monocyte derived macrophages (Fig 3A) using
15 lysotracker red, as well as lysosomal activity probes, DQ-BSA and MRC. The results (Fig 3B,
16 S3 A, B) show that naïve macrophages have a broad spread of distribution of integral
17 intensity of all the three lysosomal probes tested, indicating substantial heterogeneity
18 within the macrophage population. The distribution of bystander cells was contained within
19 the naïve cell distribution. However, the bounds of the distribution of the infected cells
20 extended beyond the upper limits of the naïve cells, showing that the alterations in
21 lysosomes are specific for infected cells. This pattern was similar at 2 and 48 hpi, indicating
22 the sustained nature of lysosomal alteration in infected macrophages (Fig 3B). Similar
23 results were obtained in THP-1 monocyte derived macrophages infected with *M. bovis* BCG
24 (Fig 3C) and stained with lysotracker red.

25
26 Next, we assessed if the alterations observed on lysosomes are specific to Mycobacterial
27 infections, since emerging literature suggests a role for lysosomal expansion during
28 phagocyte activation, including *E. coli* infection (Gray et al., 2016). Towards this, we
29 compared the lysosomal distributions with a similar experiment in *E. coli* infected
30 macrophages. The result (Fig 3D) shows that the distribution of lysosomal integral intensity
31 of *E. coli* infected macrophages, despite a relative increase compared to uninfected cells
32 immediately after infection, remained within the bounds of naïve macrophages (Fig 3D),
33 suggesting that the lysosomal response observed during Mtb infections is distinct.
34 Moreover, the classifier previously trained to predict the infection status of a cell solely
35 based on its lysosomal features failed to predict *E. coli* infected cells (Fig 3E). Together, these
36 results suggest that alteration in lysosomal homeostasis is distinct in *Mtb* infected cells, and
37 imply that *mycobacteria* specific factor(s) cause the altered lysosomal homeostasis during *M.*
38 *tuberculosis* infection.

39

40 **Mycobacterial components modulating the lysosomal pathway**

41 We hypothesized that the factor(s) modulating lysosomal homeostasis could be of
42 mycobacterial origin. We reasoned that the mycobacterial surface components could play a
43 role in the adaptive lysosomal homeostasis, since surface lipids could access the host endo-
44 lysosomal pathway and are known to be involved in virulence and modulation of host
45 responses (Beatty and Russell, 2000; Fratti et al., 2003; Vergne et al., 2004). Hence, we

1 screened different *M. tuberculosis* surface components for their effect on host lysosomes.
2 Addition of total *M. tuberculosis* lipids to THP-1 monocyte derived macrophages resulted in a
3 significant increase in cellular lysosomes, as assessed by lysotracker red staining (Fig 4A,
4 component C1). Some of the purified individual *M. tuberculosis* surface components added at
5 identical concentration resulted in elevated lysosomal levels (Fig 4A). Two of the lipids, SL-1
6 and PIM6, showed strong response, we validated them in independent assay at lower doses
7 (Fig 4 B, C). We further validated this by adding increasing amounts of SL-1 to THP-1
8 monocyte derived macrophages, which resulted in increasing levels of lysotracker red
9 fluorescent vesicles (Fig S4 A).

10
11 Next, we checked if the increase is specific for lysotracker red staining, or if lysosomal
12 activity is increased as well. Hence, we pulsed SL-1 treated THP-1 monocyte derived
13 macrophages with lysosomal activity probes DQ-BSA and MRC (Fig 4 D, E) and obtained
14 similar results showing that total cellular lysosomal content and activity increases upon SL-
15 1 treatment. The increase in lysosomal content upon SL-1 treatment was further confirmed
16 by immunoblotting lysates of SL-1 treated THP1 cells for lysosomal marker Lamp1 (Fig 4F).
17 Importantly, RAW macrophages, as well as non-macrophage cells like HeLa cells treated
18 with SL-1 showed similar phenotypes (Fig S4 B, C), showing that the increased lysosomal
19 phenotype mediated by SL-1 is not cell-type specific and suggesting that SL-1 could
20 influence a molecular pathway broadly conserved in different cell type. To assess if SL-1
21 effect is specific for lysosomes or if it influences upstream endocytic pathway, we pulsed SL-
22 1 treated cells with two different endocytic cargo, fluorescently tagged transferrin or
23 dextran. The results (Fig S4 D, E) show that SL-1 does not affect endocytic uptake suggesting
24 that its effect is specifically modulating lysosomes.

25
26 Next, we aimed to gain insights into the molecular mechanism by which SL-1 influences
27 lysosome biogenesis. The role of the mTORC1 complex in lysosomal biogenesis is well
28 known (Lawrence and Zoncu, 2019). We reasoned that if mTORC1 is involved in SL-1
29 mediated lysosomal increase, it should not have additive effect on lysosomal increase when
30 combined with Torin1, a well-known mTORC1 inhibitor (Thoreen et al., 2009). Hence, we
31 co-treated cells with Torin1 and SL-1 and, tested for any additive effect on lysosomal
32 biogenesis. The result (Fig 5A) showed that while Torin1 and SL-1 increased lysosomal
33 content in the cells individually, they did not show an additive effect when added together
34 (Fig 5 A), suggesting that SL-1 acts through mTORC1. In order to check if SL-1 influences
35 mTORC1 activity, we immunoblotted lysates from control and SL-1 treated cells with
36 antibodies specific against phosphorylated forms of the mTORC1 substrate, S6 Kinase. The
37 results show significant decrease in S6K phosphorylation, showing that SL-1 inhibits
38 mTORC1 activity (Fig 5B). Similar results were obtained with a different lysosome
39 increasing Mtb lipid PIM6 (Fig 5C) showing that different Mtb factors can act in concert
40 using similar host mechanism. mTORC1 inhibition releases the transcription factor TFEB
41 from lysosomes which translocates to the nucleus and binds to the genes containing CLEAR
42 motif, to drive the transcription of lysosomal genes (Bouché et al., 2016; Vega-Rubin-de-
43 Celis et al., 2017). Hence, we checked if SL-1 mediated inhibition of mTORC1 results in
44 nuclear translocation of TFEB. Towards this, we transfected HeLa as well as RAW cells with
45 TFEB-GFP (Roczniak-Ferguson et al., 2012) and treated with SL-1. Torin1 was used as

1 positive control in these assays. The results (Fig 5 D, S5 A) show a significant nuclear
2 translocation of TFEB upon SL-1 treatment. Finally, to confirm the involvement of TFEB in
3 SL-1 mediated increase in lysosomes, we silenced TFEB expression in THP-1 macrophages
4 with esiRNA for TFEB. Silencing was confirmed by western blotting for TFEB (Fig S5 B). We
5 treated TFEB and universal negative control (UNC) silenced cells with SL-1, and quantified
6 the change in lysosomal number between the different conditions (Fig 5 E). The result
7 shows a significant reduction in the number of lysosomes in TFEB silenced cells treated with
8 SL-1. Similar results were obtained with the positive control Torin1 (Fig 5E).

9 In the assays described above, we have treated cells with purified SL-1. The presentation of
10 lipids to the host cells, and consequently its response, can be different when added
11 externally in a purified format, or presented in the context of Mtb bacteria. Hence, we tested
12 the relevance of SL-1 mediated alteration in lysosomal homeostasis in the context of Mtb
13 infection. WhiB3 is a mycobacterial protein that controls the flux of lipid precursors through
14 the biosynthesis of lipids such as SL-1. *MtbΔWhiB3* mutants show significantly reduced
15 levels of SL-1 both *in vitro* culture and within macrophages (Singh et al., 2009). If SL-1
16 presentation from Mtb is relevant for lysosomal alterations, we expected cells infected with
17 *MtbΔwhiB3* to show reduced lysosomes relative to cells infected with wt Mtb. In order to
18 test this, we infected THP-1 cells with wild type *Mtb* H37Rv and *MtbΔwhiB3* and assessed
19 the total lysosomal content of infected macrophages by staining for lysotracker red, DQ-BSA
20 and MRC. The results (Fig S6 A-C) show that indeed cells infected with *MtbΔwhiB3* have
21 reduced lysosomal levels compared to wild type Mtb infected cells. Importantly, chemical
22 complementation of *MtbΔwhiB3* with purified SL-1 rescued the lysosomal phenotype (Fig S6
23 A-C). These results show a role for SL-1 in altering lysosomal homeostasis in the context of
24 Mtb infection. However, *MtbΔWhiB3* cells show higher lysosomal content compared to their
25 non-infected control, suggesting that additional mycobacterial factors are involved in
26 modulating lysosomal alterations.

27 WhiB3 is a transcription factor that controls Mtb redox homeostasis. While SL-1 levels are
28 reduced in *MtbΔWhiB3*, other lipids are altered as well (Singh et al., 2009), thus limiting
29 interpretation in terms of specificity to SL-1. In order to explore the direct relevance of SL-1
30 mediated increase in lysosomal biogenesis, we next used an Mtb mutant lacking polyketide
31 synthase 2 (*pks2*), a key enzyme involved in SL-1 biosynthesis pathway (Sirakova et al.,
32 2001). Infection of THP-1 macrophages with Mtb wt and *MtbΔpks2* showed that the cells
33 infected with mutant Mtb elicited a weaker lysosomal response, as assessed by lysotracker
34 red as well as the functional MRC probe staining (Fig 6 A, C). Thus, SL-1 mediates lysosomal
35 biogenesis in the context of Mtb infection. We next assessed if the reduced lysosomal levels
36 in *MtbΔpks2* infected cells affect the lysosomal delivery of Mtb. Hence, we assessed the
37 lysosomal delivery using lysosomal index as a measure of the proportion of bacteria in
38 lysosomes, as well as by directly counting the percentage of Mtb in lysosomes, using
39 lysotracker red as well as MRC labelling. The wild type Mtb, as expected and inline with our
40 earlier observation, showed a 30-40% delivery to lysosomes. Interestingly, *MtbΔpks2*
41 showed a significantly reduced delivery to lysosomes, with only ~ 20% of the mutant Mtb
42 delivered to lysosomes (Fig 6 B, C), showing that SL-1 mediated alterations in lysosomal
43 content is critical for the sub-cellular trafficking of *M. tuberculosis*. Our results with purified
44 SL-1 showed the involvement of the mTORC1-TFEB axis in modulating lysosomal

1 biogenesis. Hence, we next tested this axis in the context of *Mtb* infection. We probed lysates
2 of THP-1 monocyte derived macrophages infected with either wild type *Mtb* or *Mtb* Δ *pks2*
3 with antibody specific for phospho-4EBP1, a substrate of mTORC1. The results show a
4 significantly higher phosphorylation of 4EBP1 in mutant *Mtb* infected cells, showing a
5 relative rescue in the inhibition of mTORC1 in the absence of SL-1 (Fig 6 E). Next, we tested
6 the nuclear translocation of TFEB upon *Mtb* infection by infecting RAW macrophages
7 transfected with TFEB-GFP. The results show that similar to Torin1 treatment, wt *Mtb*
8 infection results in nuclear translocation of TFEB (Fig 6 F). Importantly, *Mtb* Δ *pks2* infected
9 cells show a partial rescue in nuclear translocation compared to wt infected cells (Fig 6F).
10 These results show that SL-1 modulates lysosomal biogenesis through the mTORC1-TFEB
11 axis in the context of *Mtb* infection.

12 Mutant *Mtb* that fail to arrest phagosome maturation are typically compromised in their
13 intracellular survival in cultured macrophages *in vitro*. In case of *Mtb* Δ *pks2*, our results show
14 a further decrease in lysosomal delivery from the wild type. In order to check if this could
15 impact intracellular *Mtb* survival, we infected THP-1 monocyte derived macrophages with
16 wt and Δ *pks2* *Mtb* and assessed intracellular bacterial survival by imaging assays, as
17 described earlier (Sundaramurthy et al., 2014; Sundaramurthy et al., 2013). The results
18 show that the number of bacteria per infected cell (Fig 6G) is significantly higher in
19 *Mtb* Δ *pks2* compared to wt *Mtb*. Finally, to confirm this phenotype, we lysed infected cells
20 and plated on 7H11 agar medium immediately after infection, or at 48 hpi, and counted the
21 number of colonies obtained. The results (Fig 6 H) show similar CFU counts immediately
22 after infection, indicating that the uptake is not altered. Importantly, at 48 hpi, significantly
23 higher number of colonies were seen in mutant bacteria infected cells (Fig 6 H) confirming
24 the higher intracellular survival of *Mtb* Δ *pks2* compared to wild type *Mtb*.

25 Next, we assessed the role of SL-1 in modulating lysosomal response *in vivo*. We infected
26 C57BL/6NJ mice with wt and *Mtb* Δ *pks2* and assessed lysosomal content in macrophages
27 obtained from single cell suspensions from infected lungs using lysotracker red and MRC
28 staining. The results shows a decreased total lysosomal content in *Mtb* Δ *pks2* infected cells
29 compared to wt *Mtb* infected cells (Fig 7 A, B) demonstrating that indeed SL-1 is involved in
30 lysosomal biogenesis also during *in vivo* infections. Despite this difference, both wt and
31 *Mtb* Δ *pks2* infected cells showed higher lysosomal content compared to their respective
32 uninfected controls based on lysotracker red and MRC staining (Fig S7 A-D), showing that
33 the redundancy in the system is also conserved *in vivo*. Importantly, under *in vivo* infection
34 conditions as well, *Mtb* Δ *pks2* showed reduced localization with lysosomal probes (Fig 7C,
35 D).

36 DISCUSSION

37 Our results here demonstrate that *Mtb* infection induces lysosomal biogenesis in
38 macrophages, which in turn controls the intracellular bacterial survival. Global alterations
39 in fundamental host cellular processes upon intracellular infections have not been
40 systematically explored. Here we report that *M. tuberculosis* infected macrophages have
41 significantly elevated lysosomal features compared to non-infected cells. Strikingly, these
42 alterations are sustained over time and conserved during *in vivo* infections, thus defining a
43 rewired lysosomal state of an infected macrophage. The alterations in lysosomes are

1 mediated by mycobacterial surface components, notably Sulfolipid-1 (SL-1). SL-1 alone
2 induces lysosomal biogenesis in a cell type independent manner by modulating the
3 mTORC1-TFEB axis of the host cells. *Mtb* Δ *pkS2*, a mutant that does not produce SL-1, shows
4 reduced lysosomal response in macrophages, resulting in reduced bacterial delivery to
5 lysosomes and increased intracellular survival. Thus, the enhanced lysosomal state of *Mtb*
6 infected cells has a host protective role, by modulating the *Mtb* delivery to lysosomes.
7

8 It is well established in *in vitro* infection models that *M. tuberculosis* blocks the maturation of
9 its phagosome to lysosome, instead residing in a modified *mycobacteria* containing
10 phagosome (Armstrong and Hart, 1971; Cambier et al., 2014; Pieters, 2008; Russell, 2001).
11 Recent reports have shown that pathogenic *mycobacteria* are delivered to lysosomes *in vivo*,
12 where they continue to survive, albeit at a reduced rate (Levitte et al., 2016; Sundaramurthy
13 et al., 2017). In the assays conditions reported in this work, both during *in vitro* and *in vivo*
14 experiments, *Mtb* remained largely outside lysosomes, inline with earlier observation that
15 *Mtb* is delivered to lysosomes *in vivo* only after an initial period of avoiding lysosomal
16 delivery (Sundaramurthy et al., 2017). Therefore, in the context of this work, majority of *Mtb*
17 are within the arrested phagosome. The maturation of phagosome requires sequential
18 fusion with endosomes, but what are the consequences of the presence of an arrested
19 phagosome on the host endo-lysosomal pathway? Few studies have systematically explored
20 such global alterations. Notably, Podinovskaia *et al* showed that in macrophages infected
21 with *M. tuberculosis*, trafficking of an independent phagocytic cargo is altered, with changes
22 in proteolysis, lipolysis and acidification rates (Podinovskaia et al., 2013), suggesting
23 alterations in the host trafficking environment beyond the confines of the mycobacterial
24 phagosome. Similarly, *M. tuberculosis* infected tissues show strong alterations in the
25 trafficking environment, which influences the trafficking of a subsequent infection
26 (Sundaramurthy et al., 2017). Thus, the environment of *M. tuberculosis* infected cells and
27 tissues are significantly different from a non-infected condition. By combining data from
28 different macrophage – *mycobacteria* infection systems, including strikingly single cell
29 isolates from *in vivo* infection, we show that this modulation is robust. In fact, the alterations
30 in lysosomes are strong enough to accurately predict an infected cell only based on the
31 lysosomal features, in the absence of any information from the bacteria. Therefore, the
32 elevated lysosomal features are distinctive and indeed a defining aspect of *M. tuberculosis*
33 infected macrophage.

34 Mycobacterial components, including surface lipids and proteins, have been observed in the
35 infected cells outside of the mycobacterial phagosome, as well as in neighboring non-
36 infected cells (Aliprantis et al., 1999; Beatty et al., 2001; Beatty et al., 2000; Beatty and
37 Russell, 2000; Dao et al., 2004; Fineran et al., 2017; Harth et al., 1994; Harth et al., 1996; Korf
38 et al., 2005; Neyrolles et al., 2001; Queiroz and Riley, 2017; Sakamoto et al., 2013; Sequeira
39 et al., 2014), where they can influence the antigen presenting capacity of macrophages or
40 interfere with other macrophage functions (Russell et al., 2002). Specifically, individual
41 mycobacterial lipids, including Phosphatidylinositol mono- and di mannosides (PIMs),
42 phosphatidylglycerol, cardiolipin, phosphatidylethanolamine, trehalose mono- and
43 dimycolates are released into the macrophage and accumulate in late endosomes/lysosomes
44 (Beatty et al., 2001; Beatty et al., 2000; Beatty and Russell, 2000; Russell et al., 2002). Our

1 comparison of lysosomal features between *mycobacteria* and other infection conditions
2 suggested that *mycobacteria* specific factors modulate lysosomal but not endosomal
3 parameters. In this study, we identify few mycobacterial surface components that increase
4 the macrophage lysosomes, even in the absence of infection, in a cell autonomous way.

5 Of the lipids tested, SL-1 showed a prominent effect on host lysosomes. Although considered
6 non-essential for mycobacterial growth in culture, SL-1 is an abundant cell wall lipid,
7 contributing up to 1-2% of the dry cell wall weight (Goren, 1970). SL-1 synthesis is
8 controlled by multiple mechanisms and is upregulated during infection of both human
9 macrophages and in mice (Asensio et al., 2006; Graham and Clark-Curtiss, 1999; Rodríguez
10 et al., 2013; Singh et al., 2009; Walters et al., 2006). Consequently, SL-1 has been proposed to
11 play multiple roles in host physiology, including modulation of secretion of pro- and anti-
12 inflammatory cytokines, phagosome maturation arrest, antigen presentation (Bertozzi and
13 Schelle, 2008; Daffé and Draper, 1998; Goren, 1972; Goren, 1990). Despite this extensive
14 literature, the exact role of SL-1 in *M. tuberculosis* pathogenesis is unclear. Here we show
15 that SL-1 influences lysosomal biogenesis by activating nuclear translocation of the
16 transcription factor TFEB in an mTORC1 dependent manner. Most of the studies attributing
17 cellular roles for individual lipids employ purified lipids; but, the abundance, distribution
18 and presentation of these lipids to the host cell from a mycobacterial cell envelope during
19 infection scenario could be different. Our results showing decreased lysosomal content in
20 macrophages infected with *Mtb* Δ *WhiB3* mutant, which is highly reduced for SL-1 (Singh et
21 al., 2009), suggests a key role for SL-1 in adaptive lysosomal homeostasis even in an
22 infection context. We further confirmed this with a SL-1 specific mutant, *Mtb* Δ *pks2*, which
23 shows the phenotype of attenuated lysosomal rewiring. Interestingly, a different SL-1
24 specific *M. tuberculosis* mutant, which lacks sulfotransferase *stf0*, the first committed
25 enzyme in the SL-1 biosynthesis pathway, shows a hyper-virulent phenotype (Gilmore et al.,
26 2012) in human macrophages. It is tempting to speculate that loss of lysosomal rewiring in
27 SL-1 mutants promotes its survival. Indeed, our results with *Mtb* Δ *pks2* confirms the hyper-
28 virulent phenotype and shows that SL-1 presentation to the host cells in the context of *Mtb*
29 influences host lysosomal biogenesis as well as phagosome maturation. Interestingly, a
30 previous study using an unbiased phenotypic high content approach has identified *Mtb*
31 mutants that over produce acetylated sulfated glycolipid (AC₄SGL) (Brodin et al., 2010).
32 These mutants show a phenotype of increased delivery to lysosomes and compromised
33 survival of the bacteria (Brodin et al., 2010). These results broadly agree with and
34 complement our observation that *Mtb* mutant lacking SL-1 show reduced delivery to
35 lysosomes and enhanced intracellular survival.

36 Silica beads coated with sulfolipid was delivered faster to lysosomes in human macrophages
37 compared to beads coated with a different lipid, showing that SL-1 alone influences
38 trafficking to lysosomes (Brodin et al., 2010). In contrast, an earlier study suggested that SL-
39 1 inhibits phagosome maturation in murine peritoneal macrophages (Goren et al., 1976).
40 These differences could be attributed to the different assays systems employed, or to the
41 intrinsic differences between human and mouse macrophages. Indeed, both *Mtb* Δ *pks2* and
42 *Mtb* Δ *stf0* do not show a survival defect in mouse and guinea pig infection models *in vivo*
43 (Gilmore et al., 2012; Rousseau et al., 2003), in contrast to their enhanced survival
44 phenotype in human macrophages. Additional compensatory mechanisms during *in vivo*

1 infections or the differential ability of human macrophages, such as production of anti-
2 microbial peptides (Gilmore et al., 2012) could contribute to these differences. Despite these
3 differences, our data shows that altered lysosomal homeostasis, mediated in part by SL-1, is
4 central to both human and mouse infection models. Clinical isolates of *Mtb* exhibit clade
5 specific virulence patterns with strong correlations of their phylogenetic relationships with
6 gene expression profiles and host inflammatory responses (Portevin et al., 2011; Reiling et
7 al., 2013; Shankaran et al., 2019). Some strains of the 'ancestral' Clade 2 show reduced
8 expression of genes in the SL-1 biosynthetic pathway (Homolka et al., 2010), while a recent
9 report shows an *Mtb* strain belonging to the ancestral lineage L1 having a point mutation in
10 the *papA2* gene, which confers it a loss of SL-1 phenotype (Panchal et al., 2019). The
11 contribution of the lysosomal alterations and their differential sub-cellular localization to
12 the distinct inflammatory responses elicited by these phylogenetically distant strains will be
13 interesting to explore.

14

15 Presence of lipids like SL-1 on the surface could provide *Mtb* with a means to regulate or fine
16 tune its own survival by modulating lysosomes and their trafficking. Generation of reliable
17 probes to accurately quantify individual lipid species such as SL-1 on the bacteria during
18 infection could play a key role in exploring this idea and enable accurate assessment of
19 variations within and across different mycobacterial strains and infection contexts. The
20 discovery that structurally unrelated lipids independently exhibit the same phenotype of
21 enhancing lysosomal biogenesis shows the redundancy in the system. Redundancy is
22 thought to confer distinct advantages to the pathogen and enable robust virulence strategies
23 without compromising on fitness (Ghosh and O'Connor, 2017). Alternatively, elevated
24 lysosomal levels could be a response of the host cells recognizing mycobacterial lipids such
25 as SL-1. Further dissection of the exact molecular targets of these lipids would be important
26 to identify host mediators involved in the process.

27

28 The success of *M. tuberculosis* depends critically on its ability to modulate crucial host
29 cellular processes and alter their function. Our results here define the elevated lysosomal
30 system as a key homeostatic feature for intracellular *M. tuberculosis* infection and uncover a
31 new paradigm in *M. tuberculosis*-host interactions: of *Mtb* and lysosomes reciprocally
32 influencing each other. Understanding the nature of this altered homeostasis and its
33 consequences for pathogenesis will enable development of effective counter strategies to
34 combat the dreaded disease.

35

36

37

38

39

1 Acknowledgements

2 VS acknowledges core funding from NCBS-TIFR, DST-Max-Planck partner group and
3 Ramalingaswamy re-entry fellowship. We thank Profs. Jean Pieters for the kind gift of *M.*
4 *bovis* expressing GFP and Marc Bickle for critical comments, Mahamad Ashiq for technical
5 assistance. We acknowledge BEI resources for providing *M. tuberculosis* components and
6 CDC1551 strains used in the study. The BSL3 facility in the Center for Infectious Disease
7 Research (CIDR), Indian Institute of Science (IISc) is gratefully acknowledged for Mtb animal
8 infections. We acknowledge the Central Imaging and Flow Cytometry (CIFF), Screening,
9 Animal house and BSL3 facilities at NCBS. The study has been approved by the Institutional
10 Animal Ethics Committee and Institutional Biosafety committees from NCBS and IISc, as well
11 as Institutional Human Ethics committee from NCBS.

12

13 The authors declare that they have no competing interests.

14

15

16 References

- 17 Aliprantis, A.O., Yang, R.B., Mark, M.R., Suggett, S., Devaux, B., Radolf, J.D., Klimpel,
18 G.R., Godowski, P., and Zychlinsky, A. (1999). Cell activation and apoptosis by
19 bacterial lipoproteins through toll-like receptor-2. *Science (New York, N.Y.)* *285*,
20 736-739.
- 21 Armstrong, J.A., and Hart, P.D. (1971). Response of cultured macrophages to
22 *Mycobacterium tuberculosis*, with observations on fusion of lysosomes with
23 phagosomes. *The Journal of experimental medicine* *134*, 713-740.
- 24 Asensio, J.G., Maia, C., Ferrer, N.L., Barilone, N., Laval, F., Soto, C.Y., Winter, N., Daffé,
25 M., Gicquel, B., Martín, C., and Jackson, M. (2006). The Virulence-associated Two-
26 component PhoP-PhoR System Controls the Biosynthesis of Polyketide-derived
27 Lipids in *Mycobacterium tuberculosis*. *Journal of Biological Chemistry* *281*,
28 1313-1316.
- 29 Beatty, W., Ullrich, H.J., and Russell, D.G. (2001). Mycobacterial surface moieties are
30 released from infected macrophages by a constitutive exocytic event. *European*
31 *Journal of Cell Biology* *80*, 31-40.
- 32 Beatty, W.L., Rhoades, E.R., Ullrich, H.J., Chatterjee, D., Heuser, J.E., and Russell, D.G.
33 (2000). Trafficking and release of mycobacterial lipids from infected macrophages.
34 *Traffic (Copenhagen, Denmark)* *1*, 235-247.
- 35 Beatty, W.L., and Russell, D.G. (2000). Identification of mycobacterial surface
36 proteins released into subcellular compartments of infected macrophages. *Infection*
37 *and immunity* *68*, 6997-7002.
- 38 Bertozzi, C.R., and Schelle, M.W. (2008). 18 Sulfated Metabolites from
39 *Mycobacterium tuberculosis*: Sulfolipid-1 and Beyond. In *The Mycobacterial Cell*
40 *Envelope (American Society of Microbiology)*, pp. 291-303.

- 1 Bouché, V., Espinosa, A.P., Leone, L., Sardiello, M., Ballabio, A., and Botas, J. (2016).
2 *Drosophila* Mitf regulates the V-ATPase and the lysosomal-autophagic pathway.
3 *Autophagy* 12, 484-498.
- 4 Breiman, L. (2001). Random Forests. *Machine Learning* 45, 5-32.
- 5 Brodin, P., Poquet, Y., Levillain, F., Peguillet, I., Larrouy-Maumus, G., Gilleron, M.,
6 Ewann, F., Christophe, T., Fenistein, D., Jang, J., *et al.* (2010). High content phenotypic
7 cell-based visual screen identifies *Mycobacterium tuberculosis* acyltrehalose-
8 containing glycolipids involved in phagosome remodeling. *PLoS Pathog* 6, e1001100.
- 9 Cambier, C.J., Falkow, S., and Ramakrishnan, L. (2014). Host Evasion and Exploitation
10 Schemes of *Mycobacterium tuberculosis*. *Cell* 159, 1497-1509.
- 11 Daffé, M., and Draper, P. (1998). The envelope layers of mycobacteria with reference
12 to their pathogenicity. *Advances in microbial physiology* 39, 131-203.
- 13 Dao, D.N., Kremer, L., Guérardel, Y., Molano, A., Jacobs, W.R., Porcelli, S.A., and Briken,
14 V. (2004). *Mycobacterium tuberculosis* lipomannan induces apoptosis and
15 interleukin-12 production in macrophages. *Infection and immunity* 72, 2067-2074.
- 16 Deretic, V. (2014). Autophagy in Tuberculosis. *Cold Spring Harbor Perspectives in*
17 *Medicine* 4, a018481-a018481.
- 18 Desjardins, M. (1994). Biogenesis of phagolysosomes proceeds through a sequential
19 series of interactions with the endocytic apparatus. *The Journal of Cell Biology* 124,
20 677-688.
- 21 Fairn, G.D., and Grinstein, S. (2012). How nascent phagosomes mature to become
22 phagolysosomes. *Trends in Immunology* 33, 397-405.
- 23 Fineran, P., Lloyd-Evans, E., Lack, N.A., Platt, N., Davis, L.C., Morgan, A.J., Höglinger, D.,
24 Tatituri, R.V.V., Clark, S., Williams, I.M., *et al.* (2017). Pathogenic mycobacteria
25 achieve cellular persistence by inhibiting the Niemann-Pick Type C disease cellular
26 pathway. *Wellcome Open Research* 1, 18.
- 27 Fratti, R.A., Chua, J., Vergne, I., and Deretic, V. (2003). *Mycobacterium tuberculosis*
28 glycosylated phosphatidylinositol causes phagosome maturation arrest. *Proceedings*
29 *of the National Academy of Sciences of the United States of America* 100, 5437-5442.
- 30 Ghosh, S., and O'Connor, T.J. (2017). Beyond Paralogs: The Multiple Layers of
31 Redundancy in Bacterial Pathogenesis. *Front Cell Infect Microbiol* 7, 467.
- 32 Gilmore, S.A., Schelle, M.W., Holsclaw, C.M., Leigh, C.D., Jain, M., Cox, J.S., Leary, J.A.,
33 and Bertozzi, C.R. (2012). Sulfolipid-1 Biosynthesis Restricts *Mycobacterium*
34 *tuberculosis* Growth in Human Macrophages. *ACS Chemical Biology* 7, 863-870.
- 35 Goren, M.B. (1970). Sulfolipid I of *Mycobacterium tuberculosis*, strain H37Rv. I.
36 Purification and properties. *Biochimica et biophysica acta* 210, 116-126.
- 37 Goren, M.B. (1972). Mycobacterial lipids: selected topics. *Bacteriological reviews* 36,
38 33-64.
- 39 Goren, M.B. (1990). Mycobacterial Fatty Acid Esters of Sugars and Sulfosugars. In
40 *Glycolipids, Phosphoglycolipids, and Sulfoglycolipids* (Boston, MA, Springer US), pp.
41 363-461.
- 42 Goren, M.B., D'Arcy Hart, P., Young, M.R., and Armstrong, J.a. (1976). Prevention of
43 phagosome-lysosome fusion in cultured macrophages by sulfatides of
44 *Mycobacterium tuberculosis*. *Proceedings of the National Academy of Sciences of the*
45 *United States of America* 73, 2510-2514.
- 46 Graham, J.E., and Clark-Curtiss, J.E. (1999). Identification of *Mycobacterium*
47 *tuberculosis* RNAs synthesized in response to phagocytosis by human macrophages

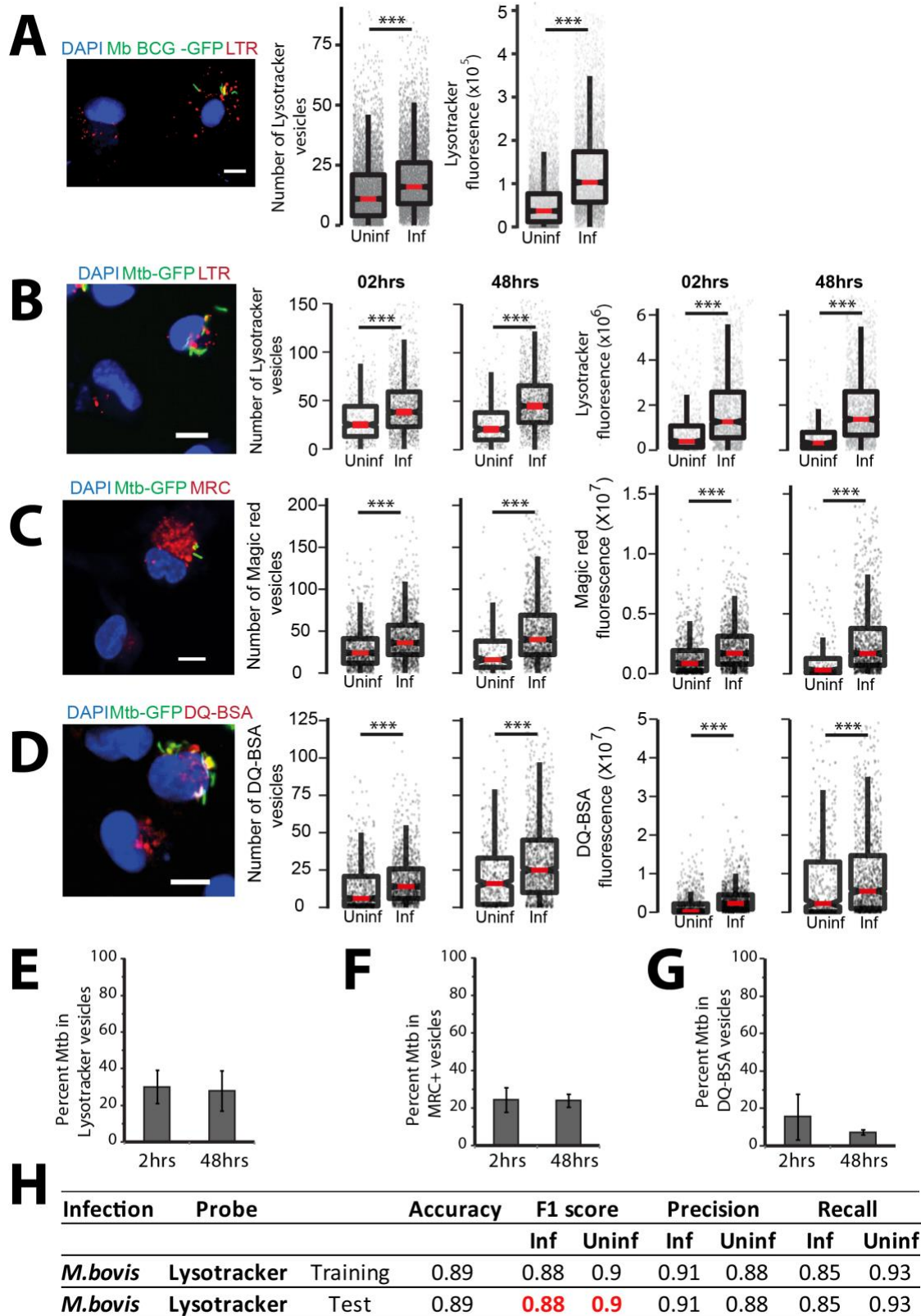
- 1 by selective capture of transcribed sequences (SCOTS). *Proceedings of the National*
2 *Academy of Sciences of the United States of America* 96, 11554-11559.
- 3 Gray, M.A., Choy, C.H., Dayam, R.M., Ospina-Escobar, E., Somerville, A., Xiao, X.,
4 Ferguson, S.M., and Botelho, R.J. (2016). Phagocytosis Enhances Lysosomal and
5 Bactericidal Properties by Activating the Transcription Factor TFEB. *Curr Biol* 26,
6 1955-1964.
- 7 Gutierrez, M.G., Master, S.S., Singh, S.B., Taylor, G.A., Colombo, M.I., and Deretic, V.
8 (2004). Autophagy Is a Defense Mechanism Inhibiting BCG and Mycobacterium
9 tuberculosis Survival in Infected Macrophages. *Cell* 119, 753-766.
- 10 Harth, G., Clemens, D.L., and Horwitz, M.A. (1994). Glutamine synthetase of
11 Mycobacterium tuberculosis: extracellular release and characterization of its
12 enzymatic activity. *Proceedings of the National Academy of Sciences of the United*
13 *States of America* 91, 9342-9346.
- 14 Harth, G., Lee, B.Y., Wang, J., Clemens, D.L., and Horwitz, M.A. (1996). Novel insights
15 into the genetics, biochemistry, and immunocytochemistry of the 30-kilodalton
16 major extracellular protein of Mycobacterium tuberculosis. *Infection and immunity*
17 64, 3038-3047.
- 18 Homolka, S., Niemann, S., Russell, D.G., and Rohde, K.H. (2010). Functional genetic
19 diversity among Mycobacterium tuberculosis complex clinical isolates: delineation
20 of conserved core and lineage-specific transcriptomes during intracellular survival.
21 *PLoS pathogens* 6, e1000988.
- 22 Korf, J., Stoltz, A., Verschoor, J., De Baetselier, P., and Grooten, J. (2005).
23 The Mycobacterium tuberculosis cell wall component mycolic acid elicits pathogen-
24 associated host innate immune responses. *European Journal of Immunology* 35, 890-
25 900.
- 26 Kumar, D., Nath, L., Kamal, M.A., Varshney, A., Jain, A., Singh, S., and Rao, K.V. (2010).
27 Genome-wide analysis of the host intracellular network that regulates survival of
28 Mycobacterium tuberculosis. *Cell* 140, 731-743.
- 29 Lawrence, R.E., and Zoncu, R. (2019). The lysosome as a cellular centre for signalling,
30 metabolism and quality control. *Nature Cell Biology* 21, 133-142.
- 31 Levin, R., Hammond, G.R.V., Balla, T., De Camilli, P., Fairn, G.D., and Grinstein, S.
32 (2017). Multiphasic dynamics of phosphatidylinositol 4-phosphate during
33 phagocytosis. *Molecular biology of the cell* 28, 128-140.
- 34 Levitte, S., Adams, K.N., Berg, R.D., Cosma, C.L., Urdahl, K.B., and Ramakrishnan, L.
35 (2016). Mycobacterial Acid Tolerance Enables Phagolysosomal Survival and
36 Establishment of Tuberculous Infection In Vivo. *Cell Host Microbe* 20, 250-258.
- 37 Lim, C.-Y., and Zoncu, R. (2016). The lysosome as a command-and-control center for
38 cellular metabolism. *The Journal of cell biology* 214, 653-664.
- 39 Neyrolles, O., Gould, K., Gares, M.P., Brett, S., Janssen, R., O'Gaora, P., Herrmann, J.L.,
40 Prévost, M.C., Perret, E., Thole, J.E., and Young, D. (2001). Lipoprotein access to MHC
41 class I presentation during infection of murine macrophages with live mycobacteria.
42 *Journal of immunology (Baltimore, Md. : 1950)* 166, 447-457.
- 43 Panchal, V., Jatana, N., Malik, A., Taneja, B., Pal, R., Bhatt, A., Besra, G.S., Thukral, L.,
44 Chaudhary, S., and Rao, V. (2019). A novel mutation alters the stability of PapA2
45 resulting in the complete abrogation of sulfolipids in clinical mycobacterial strains.
46 *FASEB BioAdvances* 1, 306-319.

- 1 Pedregosa, F., Varoquaux, G., Gramfort, A., Michel, V., Thirion, B., Grisel, O., Blondel,
2 M., Prettenhofer, P., Weiss, R., Dubourg, V., *et al.* (2011). Scikit-learn: Machine
3 Learning in Python. *Journal of Machine Learning Research*.
- 4 Pieters, J. (2008). Mycobacterium tuberculosis and the Macrophage: Maintaining a
5 Balance. *Cell Host & Microbe* 3, 399-407.
- 6 Ploper, D., and De Robertis, E.M. (2015). The MITF family of transcription factors:
7 Role in endolysosomal biogenesis, Wnt signaling, and oncogenesis. *Pharmacological*
8 *Research* 99, 36-43.
- 9 Ploper, D., Taelman, V.F., Robert, L., Perez, B.S., Titz, B., Chen, H.W., Graeber, T.G., von
10 Euw, E., Ribas, A., and De Robertis, E.M. (2015). MITF drives endolysosomal
11 biogenesis and potentiates Wnt signaling in melanoma cells. *Proc Natl Acad Sci U S A*
12 *112*, E420-429.
- 13 Podinovskaia, M., Lee, W., Caldwell, S., and Russell, D.G. (2013). Infection of
14 macrophages with Mycobacterium tuberculosis induces global modifications to
15 phagosomal function. *Cellular Microbiology* 15, 843-859.
- 16 Ponpuak, M., Davis, A.S., Roberts, E.A., Delgado, M.A., Dinkins, C., Zhao, Z., Virgin,
17 H.W., Kyei, G.B., Johansen, T., Vergne, I., and Deretic, V. (2010). Delivery of Cytosolic
18 Components by Autophagic Adaptor Protein p62 Endows Autophagosomes with
19 Unique Antimicrobial Properties. *Immunity* 32, 329-341.
- 20 Portevin, D., Gagneux, S., Comas, I., and Young, D. (2011). Human macrophage
21 responses to clinical isolates from the Mycobacterium tuberculosis complex
22 discriminate between ancient and modern lineages. *PLoS Pathog* 7, e1001307.
- 23 Queiroz, A., and Riley, L.W. (2017). Bacterial immunostat: Mycobacterium
24 tuberculosis lipids and their role in the host immune response. *Revista da Sociedade*
25 *Brasileira de Medicina Tropical* 50, 9-18.
- 26 Reiling, N., Homolka, S., Walter, K., Brandenburg, J., Niwinski, L., Ernst, M., Herzmann,
27 C., Lange, C., Diel, R., Ehlers, S., and Niemann, S. (2013). Clade-specific virulence
28 patterns of Mycobacterium tuberculosis complex strains in human primary
29 macrophages and aerogenically infected mice. *MBio* 4.
- 30 Roczniak-Ferguson, A., Petit, C.S., Froehlich, F., Qian, S., Ky, J., Angarola, B., Walther,
31 T.C., and Ferguson, S.M. (2012). The transcription factor TFEB links mTORC1
32 signaling to transcriptional control of lysosome homeostasis. *Sci Signal* 5, ra42.
- 33 Rodríguez, J.E., Ramírez, A.S., Salas, L.P., Helguera-Repetto, C., Gonzalez-y-Merchand,
34 J., Soto, C.Y., and Hernández-Pando, R. (2013). Transcription of Genes Involved in
35 Sulfolipid and Polyacyltrehalose Biosynthesis of Mycobacterium tuberculosis in
36 Experimental Latent Tuberculosis Infection. *PLoS ONE* 8, e58378.
- 37 Rousseau, C., Turner, O.C., Rush, E., Bordat, Y., Sirakova, T.D., Kolattukudy, P.E., Ritter,
38 S., Orme, I.M., Gicquel, B., and Jackson, M. (2003). Sulfolipid deficiency does not affect
39 the virulence of Mycobacterium tuberculosis H37Rv in mice and guinea pigs. *Infect*
40 *Immun* 71, 4684-4690.
- 41 Russell, D.G. (2001). Mycobacterium tuberculosis: here today and here tomorrow.
42 *Nature Reviews Molecular Cell Biology* 2, 569-578.
- 43 Russell, D.G., Mwandumba, H.C., and Rhoades, E.E. (2002). *Mycobacterium*
44 and the coat of many lipids. *The Journal of Cell Biology* 158, 421-426.
- 45 Sakamoto, K., Kim, M.J., Rhoades, E.R., Allavena, R.E., Ehrt, S., Wainwright, H.C.,
46 Russell, D.G., and Rohde, K.H. (2013). Mycobacterial trehalose dimycolate
47 reprograms macrophage global gene expression and activates matrix
48 metalloproteinases. *Infection and immunity* 81, 764-776.

- 1 Sequeira, P.C., Senaratne, R.H., and Riley, L.W. (2014). Inhibition of toll-like receptor
2 2 (TLR-2)-mediated response in human alveolar epithelial cells by mycolic acids and
3 *Mycobacterium tuberculosis* mce1 operon mutant. *Pathogens and Disease* *70*, 132-
4 140.
- 5 Settembre, C., Fraldi, A., Medina, D.L., and Ballabio, A. (2013). Signals from the
6 lysosome: a control centre for cellular clearance and energy metabolism. *Nature*
7 *Reviews Molecular Cell Biology* *14*, 283-296.
- 8 Shankaran, D., Arumugam, P., Bothra, A., Gandotra, S., and Rao, V. (2019). Modern
9 clinical *Mycobacterium tuberculosis* strains leverage type I IFN pathway
10 for a pro-inflammatory response in the host. *bioRxiv*, 594655.
- 11 Singh, A., Crossman, D.K., Mai, D., Guidry, L., Voskuil, M.I., Renfrow, M.B., and Steyn,
12 A.J.C. (2009). *Mycobacterium tuberculosis* WhiB3 Maintains Redox Homeostasis by
13 Regulating Virulence Lipid Anabolism to Modulate Macrophage Response. *PLoS*
14 *Pathogens* *5*, e1000545.
- 15 Sirakova, T.D., Thirumala, A.K., Dubey, V.S., Sprecher, H., and Kolattukudy, P.E.
16 (2001). The *Mycobacterium tuberculosis* pks2 gene encodes the synthase for the
17 hepta- and octamethyl-branched fatty acids required for sulfolipid synthesis. *J Biol*
18 *Chem* *276*, 16833-16839.
- 19 Sundaramurthy, V., Barsacchi, R., Chernykh, M., Stöter, M., Tomschke, N., Bickle, M.,
20 Kalaidzidis, Y., and Zerial, M. (2014). Deducing the mechanism of action of
21 compounds identified in phenotypic screens by integrating their multiparametric
22 profiles with a reference genetic screen. *Nature Protocols* *9*, 474-490.
- 23 Sundaramurthy, V., Barsacchi, R., Samusik, N., Marsico, G., Gilleron, J., Kalaidzidis, I.,
24 Meyenhofer, F., Bickle, M., Kalaidzidis, Y., and Zerial, M. (2013). Integration of
25 Chemical and RNAi Multiparametric Profiles Identifies Triggers of Intracellular
26 *Mycobacterial* Killing. *Cell Host & Microbe* *13*, 129-142.
- 27 Sundaramurthy, V., Korf, H., Singla, A., Scherr, N., Nguyen, L., Ferrari, G., Landmann,
28 R., Huygen, K., and Pieters, J. (2017). Survival of *Mycobacterium tuberculosis* and
29 *Mycobacterium bovis* BCG in lysosomes in vivo. *Microbes and Infection* *19*, 515-526.
- 30 Thoreen, C.C., Kang, S.A., Chang, J.W., Liu, Q., Zhang, J., Gao, Y., Reichling, L.J., Sim, T.,
31 Sabatini, D.M., and Gray, N.S. (2009). An ATP-competitive mammalian target of
32 rapamycin inhibitor reveals rapamycin-resistant functions of mTORC1. *J Biol Chem*
33 *284*, 8023-8032.
- 34 Vandal, O.H., Pierini, L.M., Schnappinger, D., Nathan, C.F., and Ehrt, S. (2008). A
35 membrane protein preserves intrabacterial pH in intraphagosomal *Mycobacterium*
36 *tuberculosis*. *Nat Med* *14*, 849-854.
- 37 Vega-Rubin-de-Celis, S., Peña-Llopis, S., Konda, M., and Brugarolas, J. (2017).
38 Multistep regulation of TFEB by MTORC1. *Autophagy* *13*, 464-472.
- 39 Vergne, I., Fratti, R.A., Hill, P.J., Chua, J., Belisle, J., and Deretic, V. (2004).
40 *Mycobacterium tuberculosis* Phagosome Maturation Arrest: *Mycobacterial*
41 Phosphatidylinositol Analog Phosphatidylinositol Mannoside Stimulates Early
42 Endosomal Fusion. *Molecular Biology of the Cell* *15*, 751-760.
- 43 Walters, S.B., Dubnau, E., Kolesnikova, I., Laval, F., Daffe, M., and Smith, I. (2006). The
44 *Mycobacterium tuberculosis* PhoPR two-component system regulates genes
45 essential for virulence and complex lipid biosynthesis. *Molecular Microbiology* *60*,
46 312-330.
- 47 Wong, C.-O., Gregory, S., Hu, H., Chao, Y., Sepúlveda, V.E., He, Y., Li-Kroeger, D.,
48 Goldman, W.E., Bellen, H.J., and Venkatachalam, K. (2017). Lysosomal Degradation Is

1 Required for Sustained Phagocytosis of Bacteria by Macrophages. *Cell Host &*
2 *Microbe* 21, 719-730.e716.
3 Yang, M., Liu, E., Tang, L., Lei, Y., Sun, X., Hu, J., Dong, H., Yang, S.-M., Gao, M., and Tang,
4 B. (2018). Emerging roles and regulation of MiT/TFE transcriptional factors. *Cell*
5 *communication and signaling : CCS* 16, 31.
6 Zhang, X., Goncalves, R., and Mosser, D.M. (2008). The isolation and characterization
7 of murine macrophages. *Curr Protoc Immunol Chapter 14*, Unit 14 11.

8
9
10
11
12
13
14
15
16
17
18
19
20
21
22
23
24
25
26
27
28
29
30



1

2 **Fig 1. *Mycobacterium tuberculosis*-infected macrophages have higher lysosomal**
 3 **content (*in vitro*).**

4 (A) Primary human macrophages infected with GFP expressing *M. bovis* BCG were pulsed
 5 with lysotracker red at 48 hpi. Number of lysotracker vesicles and integrated lysotracker

1 fluorescence intensity were compared between infected and bystander-uninfected cells. (B-
2 D) THP-1 monocyte derived macrophages were infected with *M. tuberculosis*-GFP and
3 pulsed with lysotracker red (B), MRC (C) or DQ-BSA (D) 2 and 48 hours post infection and
4 imaged. Graphs show the number and total cellular intensities of the corresponding vesicles
5 at the indicated time points. Results are representative of three or more biological
6 experiments. Statistical significance was assessed using Mann-Whitney test, *** denotes p-
7 value less than 0.001. Scale bar is 10 μ m. For A-D, data are represented as box plots, with
8 median highlighted by red line. Individual data points corresponding to single cells are
9 overlaid on the boxplots. (E-G) Differentiated THP1 macrophages were infected with *M.*
10 *tuberculosis*-GFP and pulsed with lysotracker red (E) or magic red cathepsin (F) or DQ-BSA
11 (G) to stain lysosomes at 2 and 48 hpi, fixed and imaged. Object overlap based colocalization
12 was quantified between bacteria and the respective lysosomal compartments. Bacteria
13 overlapping by more than 50% with the lysosomal compartment were considered co-
14 localised. Between 10,000 to 20,000 bacteria were analyzed for lysosomal delivery in each
15 experiment. Results are combined from three biological experiments; error bar represents
16 standard deviation between the biological replicates. (H) Multi-parametric data from
17 different infection experiments were used to train a classifier to predict infected cells based
18 on the lysosomal features, as described in methods. Test was done in the absence of
19 information on the bacteria channel. The close match in the F1 score between training and
20 test datasets indicates accurate prediction. Approximately 15,000 cells were used for the *M.*
21 *bovis* BCG training dataset, and 6500 for the test.

22

23

24

25

26

27

28

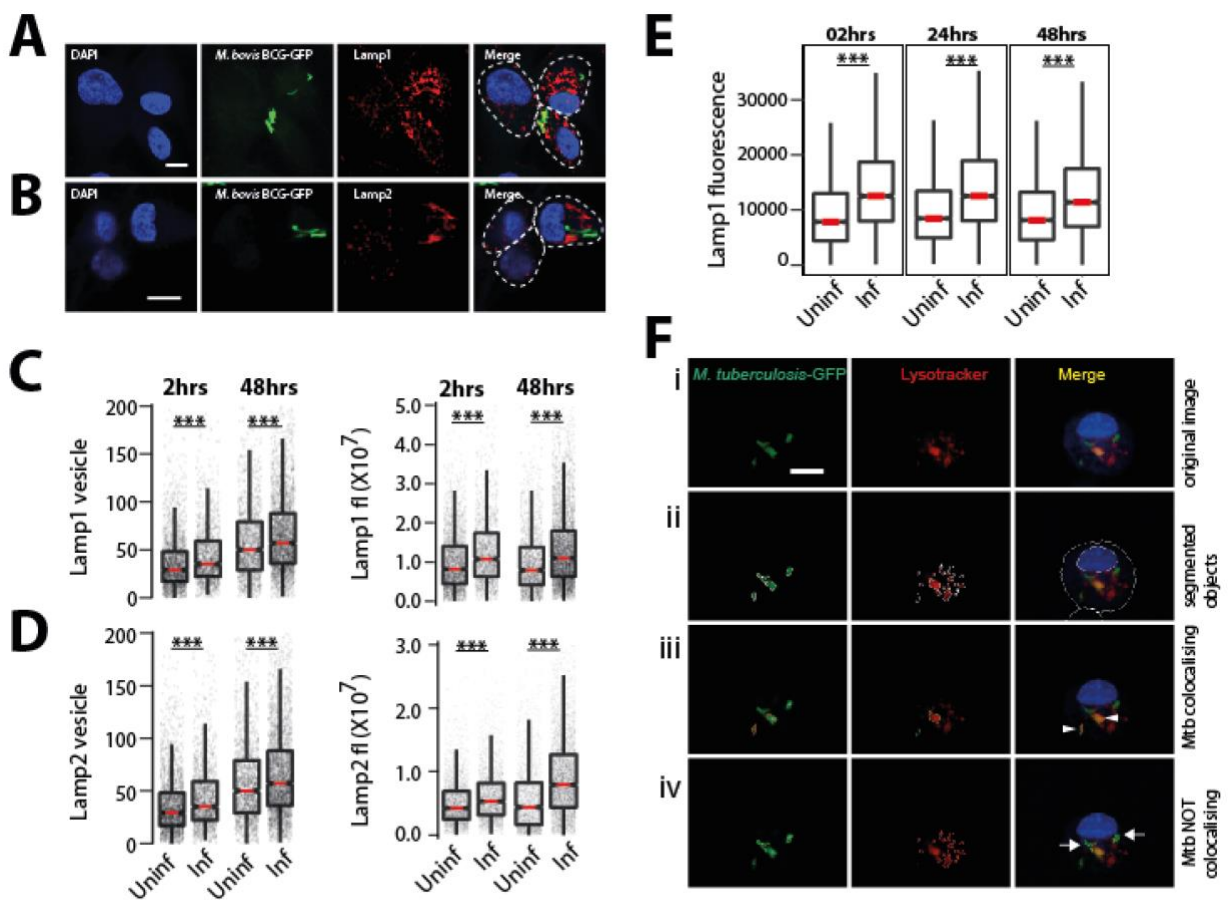
29

30

31

32

33

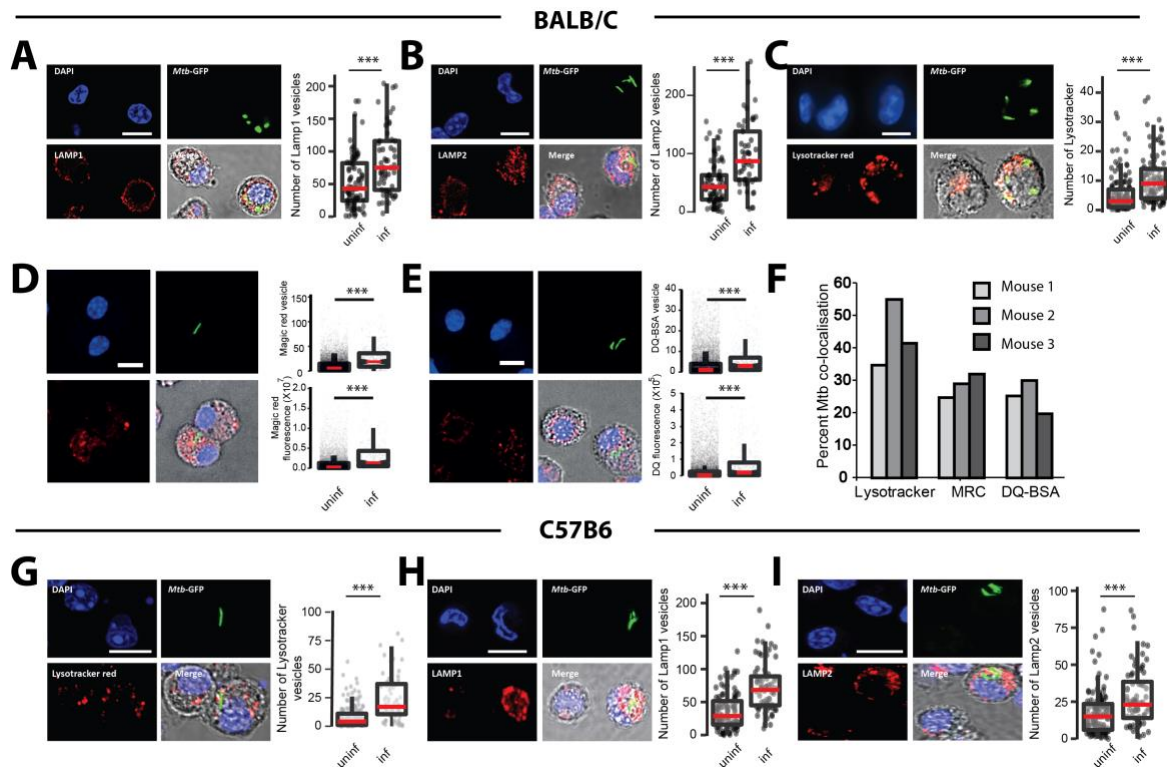


1

2 **Fig S1. *M. tuberculosis* are largely not localized to lysosomes *in vitro* in our**
 3 **experimental conditions.**

4 (A-D) Differentiated THP1 macrophages were infected with *M. bovis* BCG-GFP for 2 and
 5 48hrs, fixed and immunostained for lysosomal markers, Lamp1 (A) and Lamp2 (B). Graphs
 6 show the Lamp1 (C) and Lamp2 (D) vesicle numbers and integral intensities in infected and
 7 uninfected cells. Statistical significance was assessed by Mann-Whitney test, *** denotes p-
 8 value of less than 0.001. Data are represented as box plots, with median highlighted by red
 9 line. Individual data points corresponding to single cells are overlaid on the boxplots. (E)
 10 Differentiated THP1 macrophages were infected with *M. bovis* BCG-GFP for 2, 24 and 48hrs,
 11 fixed, immunostained for lysosomal markers, Lamp1 and analyzed by flow cytometry. Graph
 12 shows Lamp1 intensity in infected and uninfected cells at each timepoint. Approximately
 13 10000 cells were analyzed at each time point. Results are representative of three biological
 14 experiments. (F) Schematic of quantifying Mtb co-localisation with lysosomal probes. The
 15 raw image of an Mtb-GFP infected cell stained for lysotracker (i) is segmented (ii). If the
 16 segmented objects (Mtb and LTR) overlap by more than 50%, they are considered co-
 17 localised (arrow heads in panel iii), else they are not (arrows in panel iv). Object overlap
 18 based colocalization was quantified between bacteria and the respective lysosomal
 19 compartments.

20



1

2 **Fig 2. *Mycobacterium tuberculosis* infected macrophages have higher lysosomal**
 3 **content (*in vivo*).**

4 (A-C) BALB/C mice were infected with ~5000 CFUs of *M. tuberculosis*-GFP by aerosol
 5 inhalation. Four weeks post infection, macrophages were isolated from infected lungs and
 6 immunostained with Lamp1 (A), Lamp2 (B) or stained with Lysotracker red (C) and number
 7 of lysosomes were compared between infected and uninfected cells. Data are pooled from
 8 four mice. (D, E) BALB/C mice were infected with ~500 CFUs of *M. tuberculosis*-GFP by
 9 aerosol inhalation. Macrophages isolated from six weeks post infection from infected lungs
 10 and stained with magic red cathepsin (D) or DQ-BSA (E) and lysosome number and integral
 11 intensity was compared between infected and uninfected cells. Data are pooled from three
 12 mice. Results are representative of three independent infections. Statistical significance was
 13 assessed using Mann-Whitney test, denotes p-value less than 0.001. Scale bar is 10 μ m. (F)
 14 Infected macrophages from mice lungs were isolated and pulsed with the indicated
 15 lysosomal probes (lysotracker red, magic red cathepsin and DQ-BSA). Graph shows the
 16 percentage of *M. tuberculosis* co-localising with different lysosomal probes (lysotracker red,
 17 magic red cathepsin and DQ-BSA). Data are shown separately from three individual mice.
 18 Between 100 to 250 bacteria from each mouse were analysed for lysosomal delivery.
 19 (G-I) C57BL/6J mice were infected with ~5000 CFUs of *M. tuberculosis*-GFP by aerosol
 20 inhalation and four weeks post infection macrophages were isolated from infected lungs.
 21 Panels G, H, I show representative images from Lysotracker red, Lamp1 and Lamp2 staining,
 22 respectively, of these macrophages. Data are pooled from three mice. Results are
 23 representative of two independent infections with at least three mice each. Statistical
 24 significance was assessed using Mann-Whitney test, and denotes p-value less than 0.001.
 25 Scale bar is 10 μ m. For panels A to E and G to I, data are represented as box plots, with
 26 median highlighted by red line. Individual data points corresponding to single cells are
 27 overlaid on the boxplots.

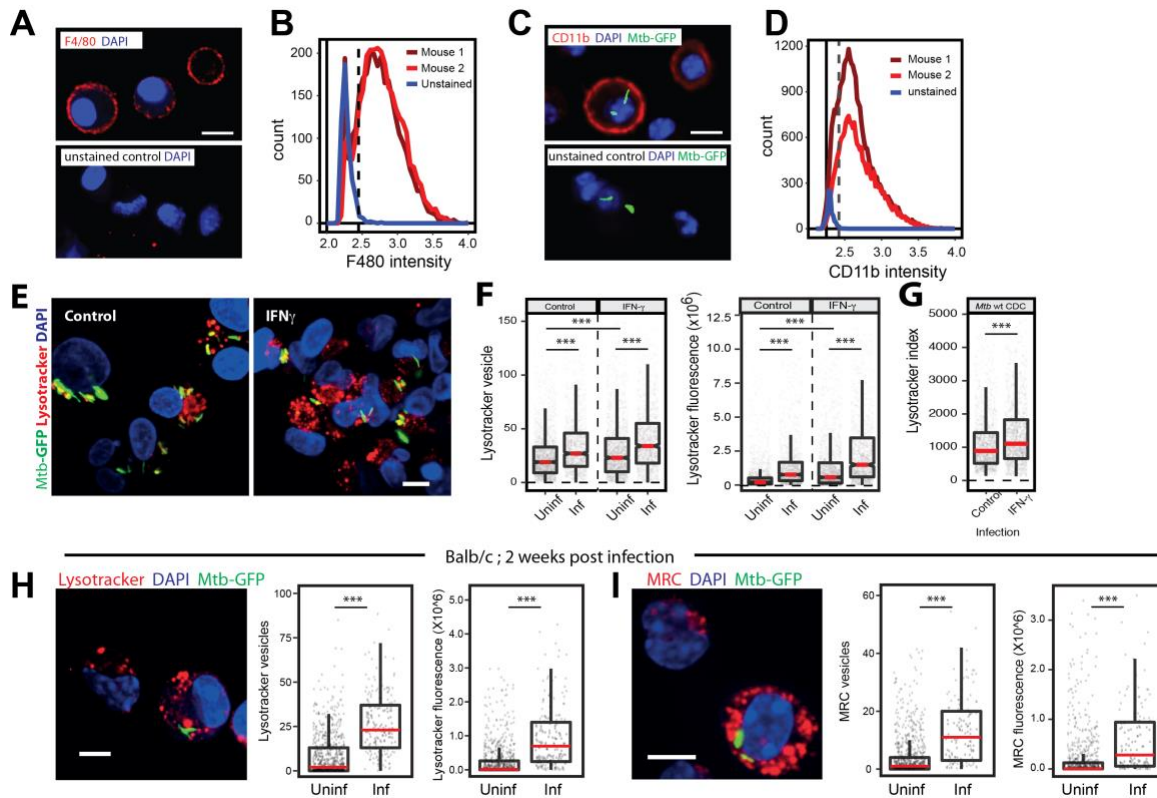
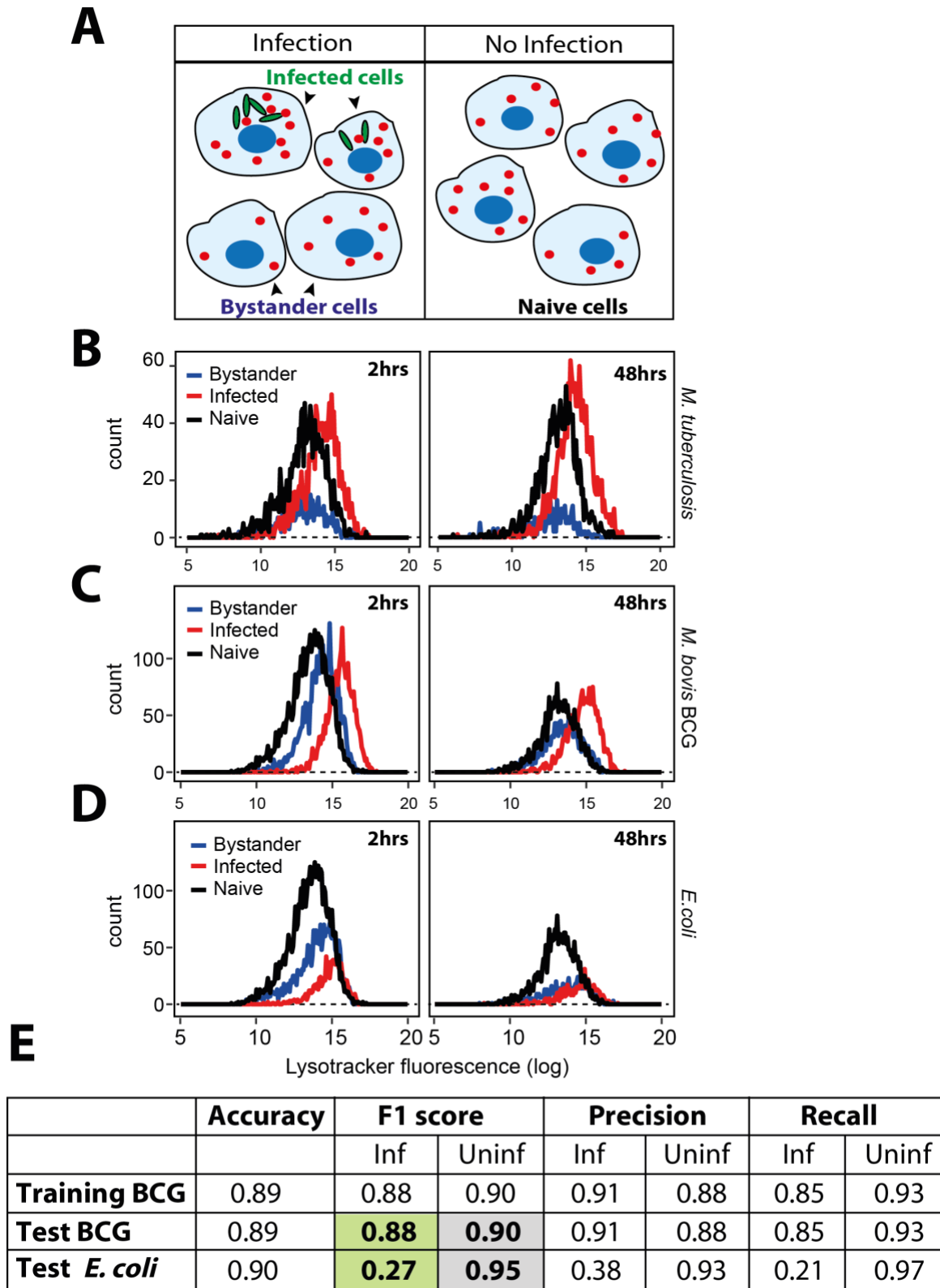


Fig S2. *M. tuberculosis* induced lysosomal increase *in vivo* is independent of adaptive immunity.

(A-D) Single-cell suspension from the lungs of infected mice were prepared and macrophages were selected by adherence for 2 hours. Non-adhered cells were washed and purity of macrophage post adherence was assessed by immunostaining with anti-F4/80 (A) or anti Cd11b (C) followed by imaging. Control i.e. unstained cells were used to determine the cut off for F4/80 or Cd11b positive population. A false-positive rate of 2-3% was used as a cut-off to determine the proportion of F4/80 or Cd11b positive cells. (B, D) Distributions are drawn from 2,500-3,000 cells per mouse, data shown from 2 mice in each experiment and are representative of at least two independent infections. Scale bar: 10 μ m. (E-G) THP1 monocyte-derived macrophages were infected with wild type CDC1551 *M. tuberculosis*-GFP followed by incubation with or without IFN-gamma (25ng/ml) containing media for 48hrs. Post 48hrs incubation, cells were stained with lysotracker red. Images (E) and graphs (F) show the number and intensity of lysotracker in control and Interferon-gamma treated infected and uninfected-bystander macrophages. (G) LysoTracker index shows intensity of lysotracker in mycobacterial phagosome in both control and treated conditions. Results are representative of three biological experiments. (H, I) BALB/C mice were infected with ~150 CFUs of *M. tuberculosis*-GFP by aerosol inhalation. 17 days post-infection, macrophages were isolated from infected lungs by making single-cell suspension and stained with lysotracker red (H) or magic red cathepsin (I) and number and intensity of lysosomes were compared between infected and uninfected cells. Results are representative of one biological infection with three mice. Statistical significance was assessed using Mann-Whitney test, *** denotes p-value of less than 0.001. Scale bar is 10 μ m. For panels F to I, data are represented as box plots, with median highlighted by red line. Individual data points corresponding to single cells are overlaid on the boxplots.



1

2 **Fig 3. *M. tuberculosis* infected macrophages show distinct lysosomal modulation**
 3 **compared to *E. coli* infected macrophages.**

4 (A) Schematic showing the experimental design to differentiate between bystander-
 5 uninfected and naïve cells. Two different wells from a multi-well plate are shown; one is
 6 infected with GFP expressing *mycobacteria*, where infected and bystander-(uninfected) cells

1 are present. Bacteria are not added to the second well, hence the cells are called unexposed-
2 naive cells. Lysosomes are illustrated in red. (B) THP-1 monocyte-derived macrophages
3 were infected with *M. tuberculosis*-GFP and stained for lysotracker red at 2 and 48 hpi. Cells
4 were fixed and imaged. Histograms compare the distribution of lysotracker intensities
5 between *M. tuberculosis*-GFP infected, bystander-uninfected and unexposed (naive)
6 macrophages at 2 and 48 hpi. Results are representative of more than three biological
7 experiments. (C, D) THP-1 monocyte-derived macrophages were infected with either *M.*
8 *bovis* BCG (C) or *E. coli* (D) and pulsed with lysotracker red at 2 and 48 hours post infection.
9 Integrated lysotracker intensity was measured between infected and uninfected cells (red
10 and blue lines) and compared to the distribution of naive macrophages (black). More than
11 800 cells were analysed of each condition for distributions. Results are representative of at
12 least two biological experiments. (E) Multiple lysosomal features from THP-1 monocyte-
13 derived macrophages infected with *M. bovis* BCG-GFP were used as a training dataset to
14 classify an infected cell solely based on lysosomal parameters (in the absence of any
15 information on the bacteria), as described in methods. Test BCG and Test *E. coli* show the
16 accuracy of the prediction, as assessed by the F1 score, precision and recall values.
17 Uninfected cells from *E. coli* and *M. bovis* BCG-GFP infected macrophage populations were
18 indistinguishable from each other in terms of the lysosomal properties; however, the
19 respective infected cells were very different. Over 7000 cells were used for the training
20 dataset, and 10,000 cells were used for test dataset for *M. bovis* BCG-GFP and *E. coli*
21 infections, respectively.

22

23

24

25

26

27

28

29

30

31

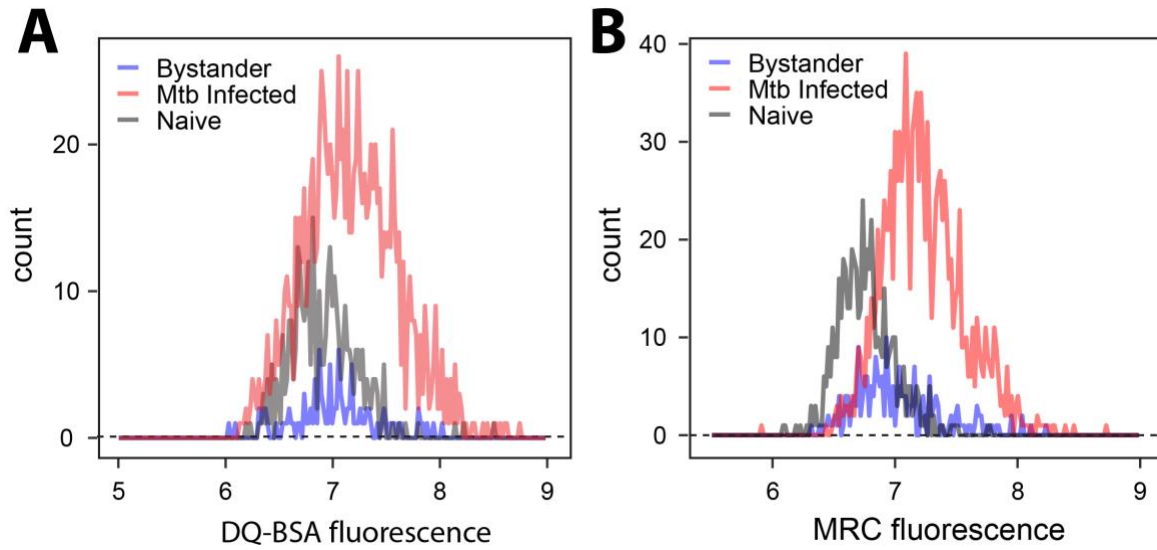
32

33

34

35

36



1

2

3 **Fig S3. *M. tuberculosis* infected macrophages have higher lysosomal activity compared**
4 **to naïve macrophages (*in vitro*).**

5 (A, B) THP-1 derived macrophages were infected with *M. tuberculosis*-GFP and lysosomes
6 were stained with lysosomal activity probes (DQ-BSA and MRC) at 48 hpi. Cells were fixed
7 and imaged. Employing image analysis per cell intensity of the respective probes was
8 measured. Histograms of single-cell intensity measurements were plotted to compare the
9 distribution of DQ-BSA and MRC intensities between *M. tuberculosis*-GFP infected,
10 uninfected and unexposed (naïve) macrophages at 48hpi post-infection. More than 1000
11 infected, 200 uninfected and 500 unexposed-naïve cells were analyzed for the distributions.
12 Results are representative of at least three biological experiments.

13

14

15

16

17

18

19

20

21

22

23

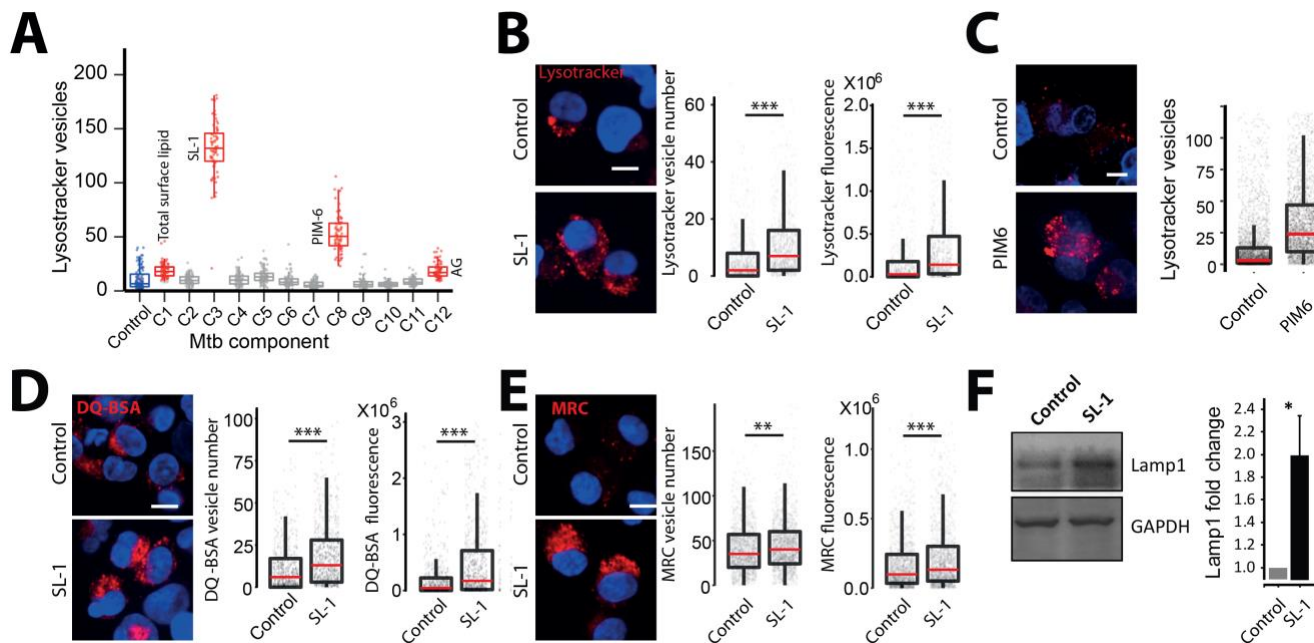


Fig 4. Mycobacterial surface lipids, predominantly SL-1, mediate alterations in host cell lysosomes.

(A) THP1 monocyte-derived macrophages were treated with different purified *M. tuberculosis* surface components at 50µg/ml concentration and screened for their effect on macrophage lysosomal content. DMSO is used as vehicle control. The *M. tuberculosis* surface components used are C1 (Total lipid), C2 (Mycolic acid), C3 (Sulfolipid-1), C4 (Trehalose Dimycolate), C5 (Mycolylarabinogalactan-Peptidoglycan), C6 (Lipomannan), C7 (Phosphatidylinositol mannosides 1 & 2), C8 (Phosphatidylinositol mannosides 6), C9 (Lipoarabidomannan), C10 (Mycobactin), C11 (Trehalose monomycolate), C12 (Arabinogalactan). Results are representative of two independent screens.

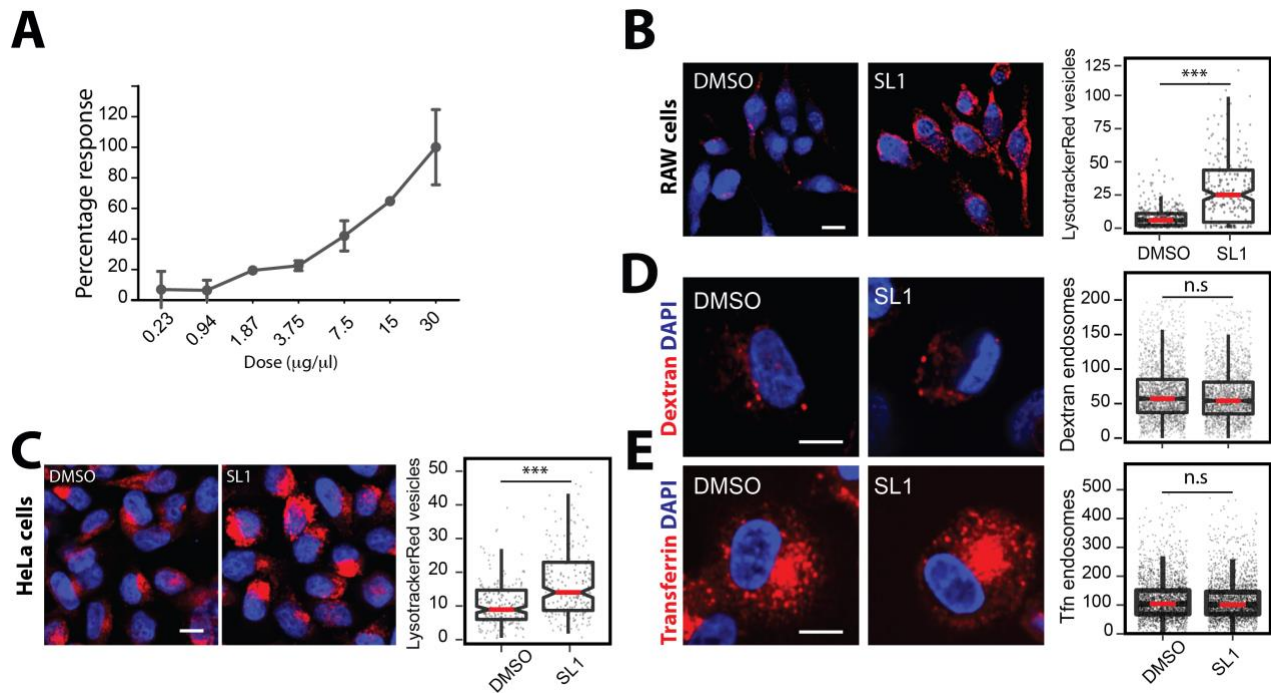
(B, C) Differentiated THP1 macrophages were treated with 20µg/ml purified SL-1 (B) or PIM6 (C) for 24hrs and stained with lysotracker red. Representative images show staining of lysotracker red in vehicle and SL-1/PIM6 treated THP-1 monocyte-derived macrophages.

(D, E) THP1 monocyte-derived macrophages were treated with 20µg/ml purified SL-1 for 24hrs and stained with lysosomal activity probes DQ-BSA (D) or MRC (E). Representative images show the staining and quantification of lysosomal number and integral intensity in respective stain in control and SL-1 treated macrophages. Statistical significance for (A-E) was assessed using Mann-Whitney test, ** denotes p-value of less than 0.001. Scale bar is 10 µm. For B-G, data are represented as box plots, with the median denoted by red line.

(F) Lamp1 protein levels in SL-1 treated THP-1 monocyte-derived macrophage lysates assessed by immunoblotting for the Lamp1 antibody. GAPDH used as a loading control. Graph shows the average and standard error of band intensity normalized to GAPDH from three or more independent experiments. Significance is assessed using unpaired-one tailed T-test with unequal variance, * represent p-value less than 0.05.

27

28



1

2 **Fig S4. Characterization of SL-1 mediated lysosomal expansion.**

3 (A) THP1 monocyte-derived macrophages were treated with different doses of purified SL-1
4 (0.23-30 $\mu\text{g}/\text{ml}$) for 24hrs, pulsed with lysotracker red, fixed and imaged. DMSO was used as
5 vehicle control. Graph represents percent increase in lysotracker intensity in cell with an
6 increasing dose of SL-1 compared to DMSO control. Average and standard deviation of
7 technical replicates is shown in the graph. Results are representative of two independent
8 dose curves. (B, C) RAW macrophages (B) or HeLa cells (C) were treated with 25 $\mu\text{g}/\text{ml}$
9 purified SL-1 for 24hrs, stained with lysotracker red, fixed and imaged. Representative
10 images and quantification of lysotracker red vesicles in DMSO or SL-1 treated RAW and
11 HeLa cells are shown. (D, E) THP1 monocyte-derived macrophages were treated with
12 25 $\mu\text{g}/\text{ml}$ purified SL-1 for 24hrs, pulsed with fluorescently labeled dextran or Transferrin
13 (Tfn), fixed and imaged. Representative images and quantification of dextran and Tfn
14 endocytosis in SL-1 treated THP1 monocyte-derived macrophages are shown. Results are
15 representative of two or more biological experiments. Statistical significance was assessed
16 using Mann-Whitney test, ns denotes non-significant. Scale bar is 10 μm . For B-E, data are
17 represented as box plots, with the median denoted by red line. Individual data points
18 corresponding to single cells are overlaid on the box plot.

19

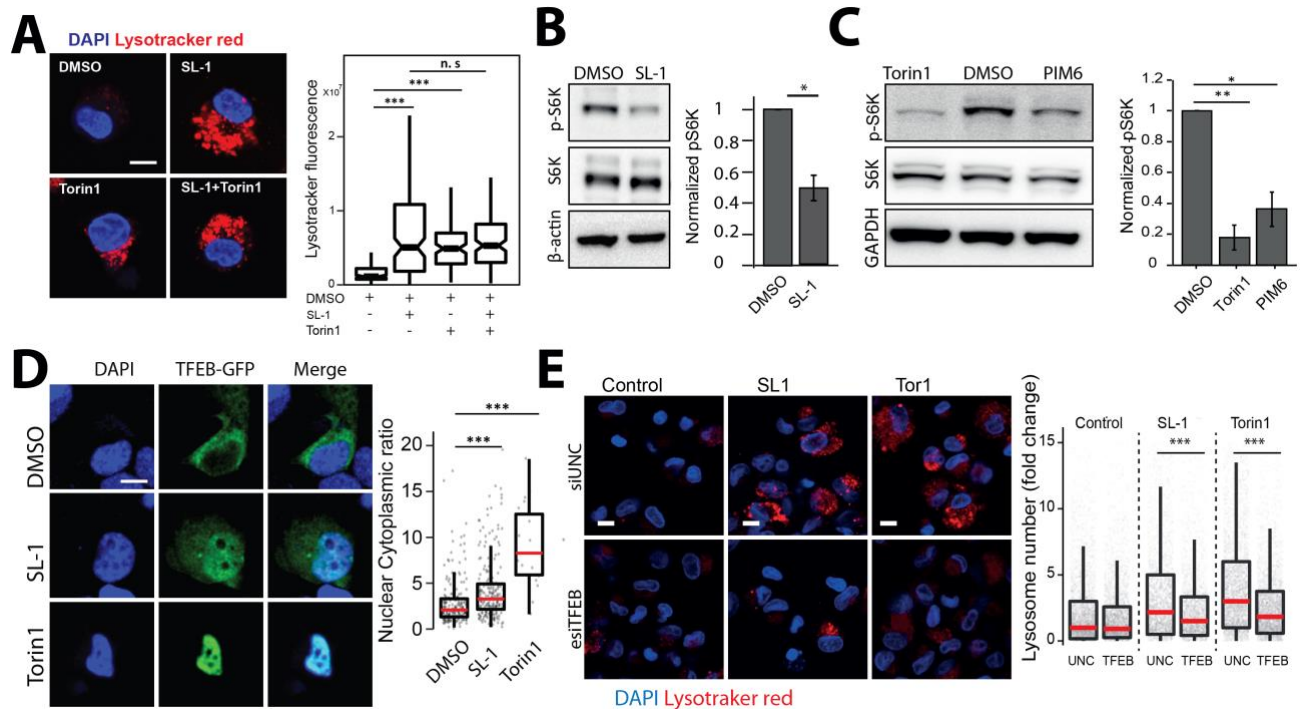
20

21

22

23

24



1
2

Fig 5. Sulfolipid-1 (SL-1) from *M. tuberculosis* influences lysosomal biogenesis in host cells via mTORC1 dependent nuclear translocation of the transcription factor EB (TFEB).

(A) Differentiated THP-1 macrophages were treated with DMSO/SL1/Torin1/SL1+Torin1 comparing lysotracker staining levels between the different conditions. Representative images and quantification of cells treated with 25 μ g/ml SL-1 and 1 μ M Torin1. Approximately 100 cells were analyzed per category in each experiment and significance assessed by Mann-Whitney test. Data presented is representative of two independent experiments. Scale bar is 10 μ m. (B, C) Immunoblots and quantification of phosphorylated and total levels of indicated proteins in THP-1 monocyte-derived macrophage lysates treated with DMSO (control) or SL-1 (B) or PIM6 (C). Torin1 (1 μ M) was used as a positive control. Bar graphs show average of at least three biological replicates and error bars represent standard deviation. Change in phosphorylation status of indicated protein (S6 Kinase) is assessed by normalizing phosphorylated protein to the respective total protein. Actin/GAPDH was used as the loading control. Significance is assessed using unpaired-one tailed T-test with unequal variance, * represent p-value less than 0.05 and ** less than 0.01. (D) RAW macrophages were transfected with TFEB-GFP for 24 hours and treated with 25 μ g/ml SL-1, or negative and positive controls, DMSO and Torin1 (250nM) respectively. Representative images and quantification of nuclear to cytoplasmic ratio of TFEB-GFP between the different conditions are shown. Results are representative of at least three independent experiments. (E) Differentiated THP1 macrophages were transfected with either control siRNA (Universal negative control 1- UNC1) or TFEB siRNA for 48hrs followed by treatment with SL-1 (25 μ g/ml for 24hrs) or Torin1 (1 μ M for 4hrs) and were pulsed with lysotracker red and imaged. Representative images and quantification of control, SL-1 and torin1 treatment in UNC1 or TFEB siRNA transfected macrophages are shown. Results

1 are representative of two biological experiments. Statistical significance for A, D and E was
2 assessed using Mann-Whitney test, and *** denotes p-value of less than 0.001. Scale bar is
3 10 μm . For A, D, E, data are represented as box plot. Individual datapoints overlaid on the
4 box plot in D and E represent single cells.

5

6

7

8

9

10

11

12

13

14

15

16

17

18

19

20

21

22

23

24

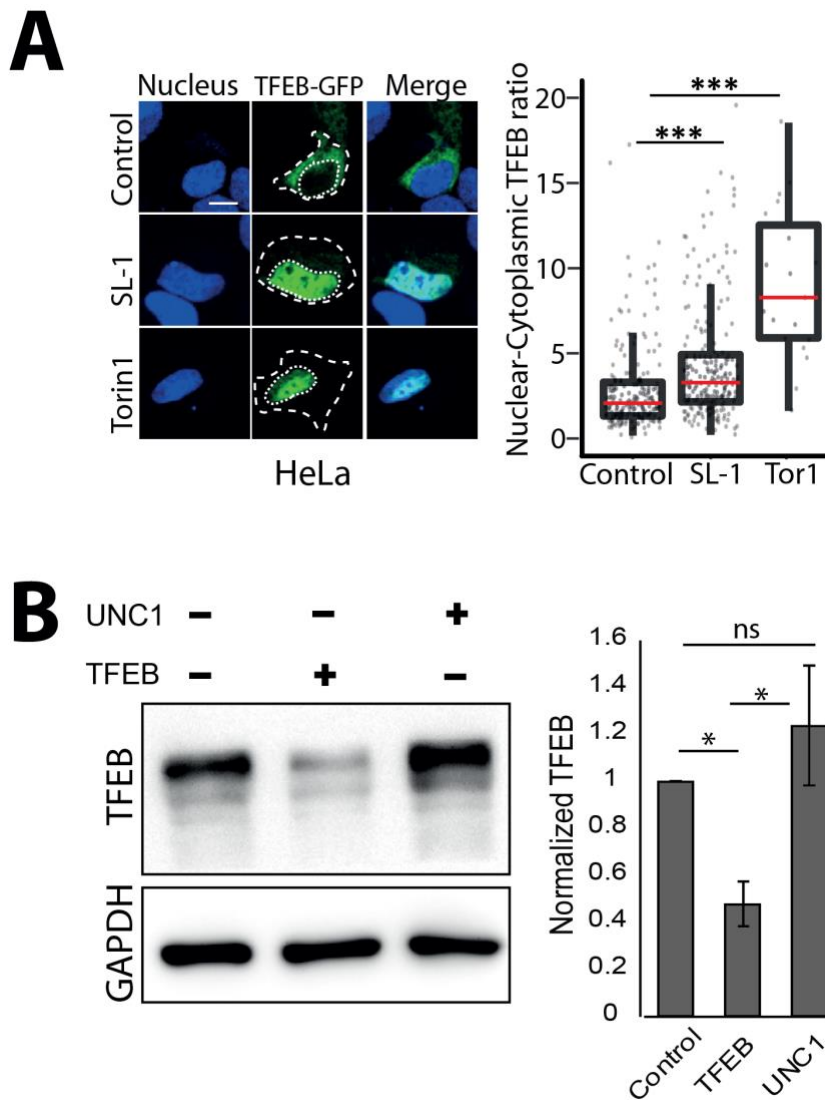
25

26

27

28

29

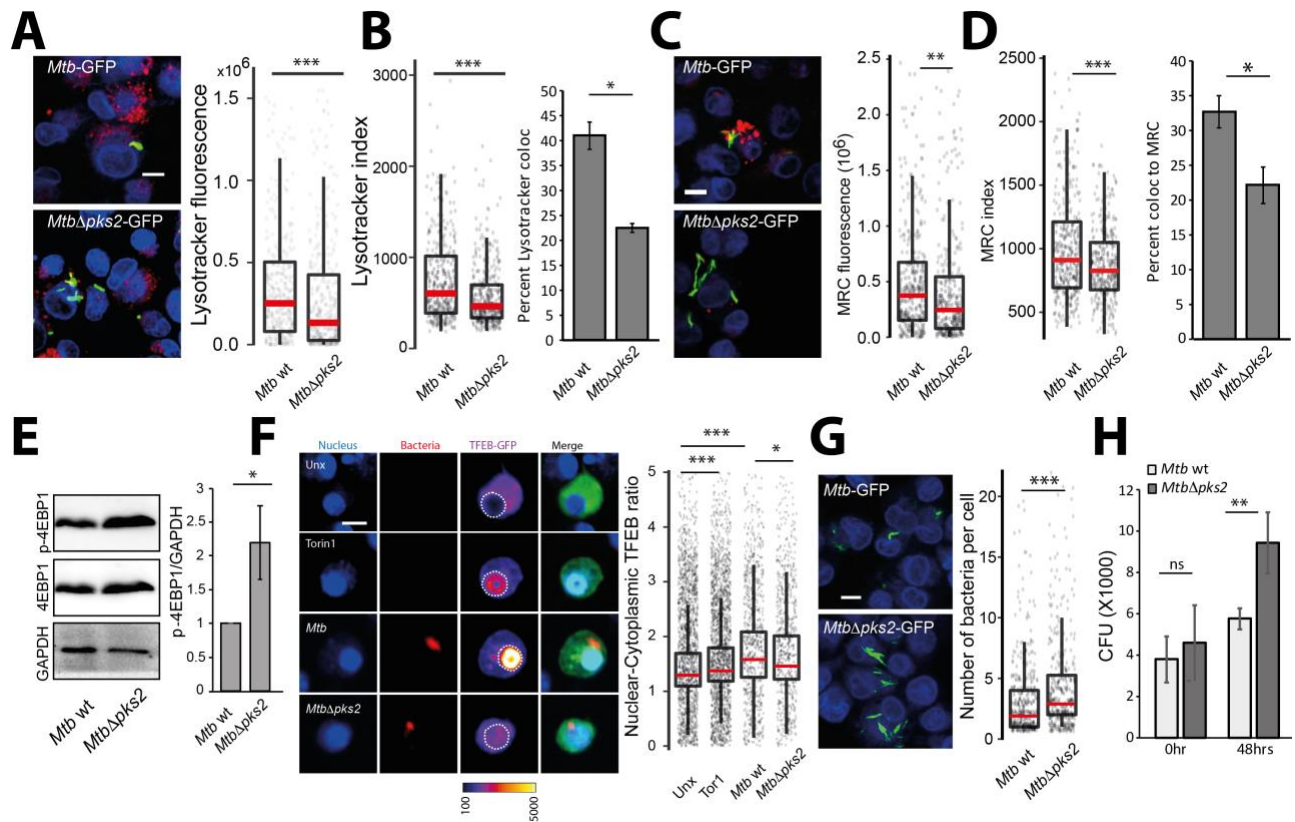


1
2
3
4
5
6
7
8
9
10
11
12
13
14
15
16
17

Fig S5. Sulfolipid-1 (SL-1) from *M. tuberculosis* influences lysosomal biogenesis in host cells via mTORC1 dependent nuclear translocation of the transcription factor EB (TFEB).

(A) HeLa cells were transfected with TFEB-GFP for 24 hours and treated with 25 μ g/ml SL-1, or negative and positive controls, DMSO and Torin1 (250 nM) respectively. Representative images and quantification of nuclear to cytoplasmic ratio of TFEB-GFP between the different conditions are shown. Results are representative of at least three biological replicates.

Statistical significance was assessed using Mann-Whitney test, *** denotes p-value of less than 0.001. Scale bar is 10 μ m. (B) Differentiated THP1 macrophages were transfected with either control (UNC1) or TFEB siRNA using lipofectamine RNAimax and TFEB knockdown efficiency was assessed by measuring TFEB protein levels post 48 hours of transfection. GAPDH was used as the loading control. Bar graph shows the average and standard error of three biological experiments. Significance is assessed using unpaired-one tailed T-test with unequal variance, and represent p-value less than 0.05.



1

2 **Fig 6. Sulfolipid-1 restricts the intracellular growth of *M. tuberculosis* by elevating**
 3 **lysosomal levels in macrophages.**

4 (A-D) THP1 monocyte-derived macrophages were infected with *Mtb* wt and *Mtb*Δ*pks2*
 5 CDC1551 *M. tuberculosis*-GFP for 48hrs and stained with different lysosome probes, namely
 6 lysotracker red (A, B), and magic red cathepsin (MRC) (C, D). Images and graphs in A and C
 7 show a comparison of the total lysosomal intensities of the respective probes in individual
 8 *Mtb* wt and *Mtb*Δ*pks2* mutant infected cells. Lysotracker (B) and MRC (D) index represent
 9 intensity of the respective probe in wt and *pks2* mutant mycobacterial phagosome.
 10 Statistical significance was assessed using Mann-Whitney test, denotes p-value of less than
 11 0.01 and * denotes p-value of less than 0.001. Results are representative of three biological
 12 experiments. Bar graphs in (B) and (D) show object-based colocalization of bacterial
 13 phagosomes with lysosomes stained with the respective lysosomal probe. Bacteria
 14 overlapping by more than 50% with the lysosomal compartment were considered co-
 15 localised. More than 1000 phagosomes were analyzed in each experiment for colocalization
 16 analysis. Results are the average of three biological experiments and standard error
 17 between the biological replicates. Significance is assessed using unpaired-one tailed T-test
 18 with unequal variance, * represent p-value less than 0.05. (E) THP1 monocyte-derived
 19 macrophages were infected with *Mtb* wt or *Mtb*Δ*pks2* CDC1551 for 48hrs. Immunoblots and
 20 quantification of phosphorylated and total 4E-BP1 are shown. GAPDH is used as loading
 21 control. Results represent the average and standard error of four biological experiments. (F)
 22 RAW macrophages were transfected with TFEB-GFP followed by 4hrs infection with *Mtb* wt
 23 or *Mtb*Δ*pks2*. Cells were fixed 4hpi, imaged and nuclear to cytoplasmic ratio of TFEB-GFP
 24 was compared between unexposed, torin1 treated, wt and *pks2* mutant infected cells. Torin1
 25 treatment (250nM for 4hrs) was used as positive control. TFEB-GFP channel images are

1 shown in Fire LUT for better visualization of the fluorescence intensities. Data points are
2 pooled from two independent biological experiments. (G) THP1 monocyte-derived
3 macrophages were infected with *Mtb* wt or *Mtb* Δ *pks2* *M. tuberculosis*-GFP for 48hrs, fixed
4 and imaged. Images and boxplot show the number of bacteria per cell for the two conditions.
5 (H) CFUs of *Mtb* wt or *Mtb* Δ *pks2* infected THP1 monocyte-derived macrophages
6 immediately after infection and 48 hours post infection. Results are the average and
7 standard error of data compiled from three biological experiments, each containing four
8 technical replicates. Significance is assessed using unpaired-one tailed T-test with unequal
9 variance, ** represent p-value less than 0.01 and ns represents non-significant. For A, C, F, G,
10 scale bar is 10 μ m, data are represented as box plots, with individual data points
11 corresponding to single cells overlaid.

12

13

14

15

16

17

18

19

20

21

22

23

24

25

26

27

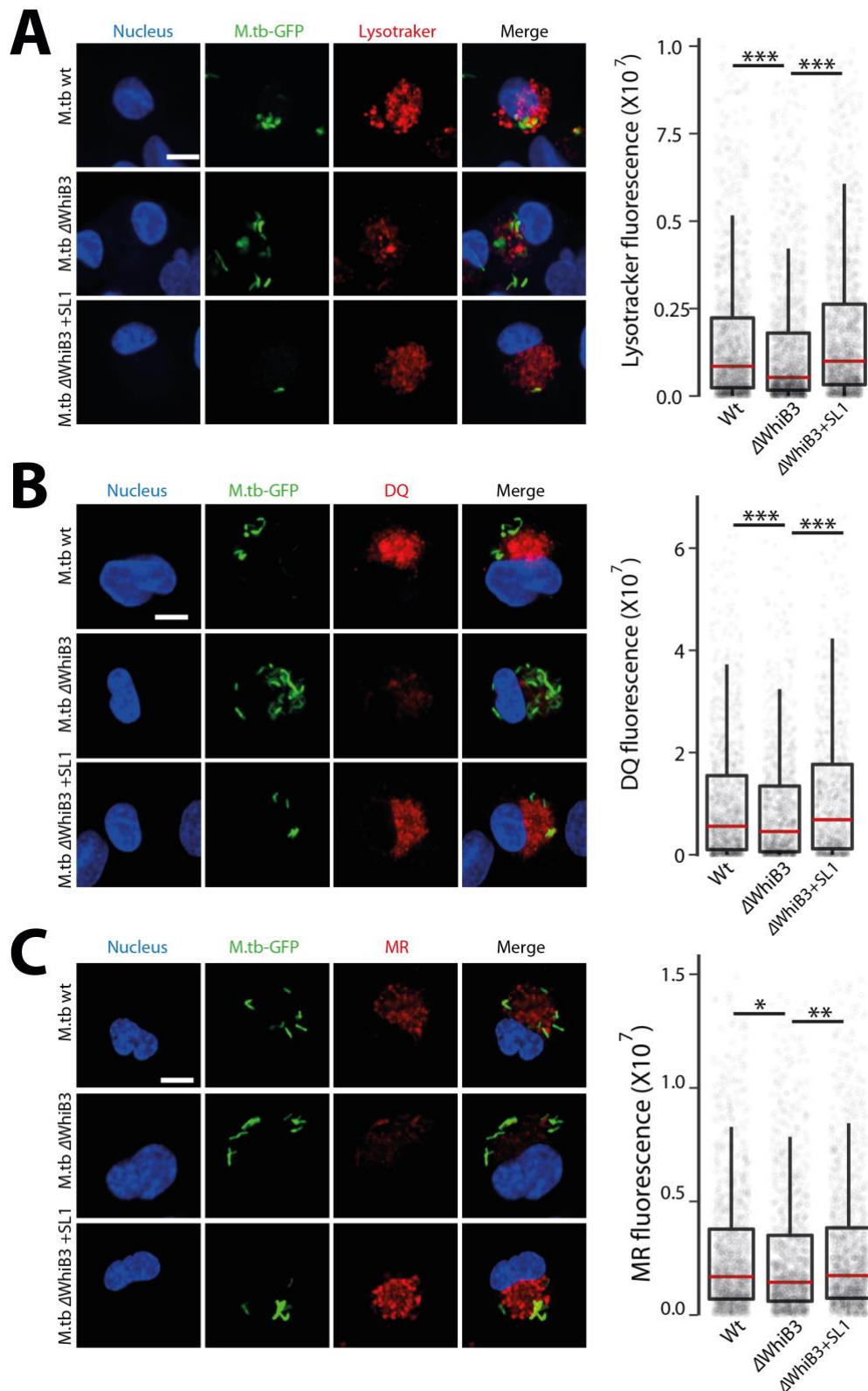
28

29

30

31

32



1

2 **Fig S6. *M.tb*ΔWhiB3 mutant infected cells show reduced lysosomal response compared**
3 **to wt *M.tb* infected cells.**

4 (A-C) THP1 monocyte-derived macrophages were infected with *M.tb* wt or *M.tb*ΔwhiB3 for
5 48hrs and stained for different lysosome probes, namely lysotracker red (A), DQ-BSA (B)

1 and magic red cathepsin (MRC) (C). Graphs show the total lysosomal intensities of the
2 respective probes in individual infected cells. $\Delta WhiB3$ +SL1 denotes *M. tuberculosis* $\Delta WhiB3$
3 infected cells complemented with 5 μ g/ml purified SL-1 for 48hrs. Results are representative
4 of three biological experiments. Statistical significance was assessed using Mann-Whitney
5 test, *** denotes p-value less than 0.001. Scale bar is 10 μ m.

6

7

8

9

10

11

12

13

14

15

16

17

18

19

20

21

22

23

24

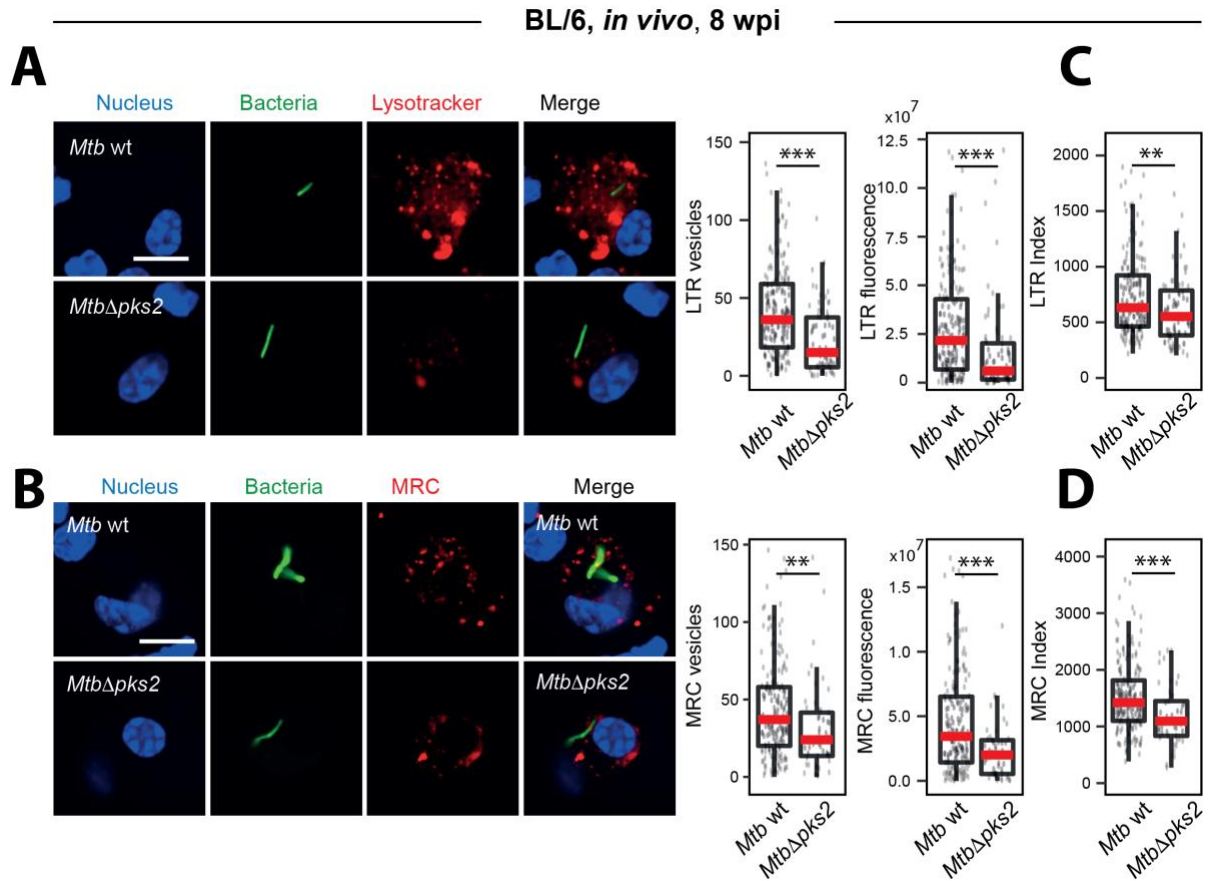
25

26

27

28

29



1

2 **Fig7. SL-1 mediated lysosomal alterations in *Mtb* infections *in vivo*.**

3 (A-D) C57BL/6N] mice were infected with *Mtb wt* or *MtbΔpks2* CDC1551 by aerosol
 4 inhalation. Eight weeks post-infection, macrophages were isolated from infected lungs from
 5 single-cell suspension and were pulsed with lysosomal probes, namely lysotracker red (A,
 6 C), and magic red cathepsin (MRC) (B, D). Number and intensity of lysosomes in respective
 7 probes were compared between *Mtb wt* or *MtbΔpks2* CDC1551 infected cells. Lysotracker
 8 red (C) and MRC (D) index represent the intensity of the respective probe in *Mtb wt* or
 9 *MtbΔpks2* CDC1551 containing phagosomes. Results are compiled from four wild type *Mtb*
 10 and three *MtbΔpks2* infected mice. Statistical significance was assessed using Mann-Whitney
 11 test, *** denotes p-value of less than 0.001. Scale bar is 10 μ m.

12

13

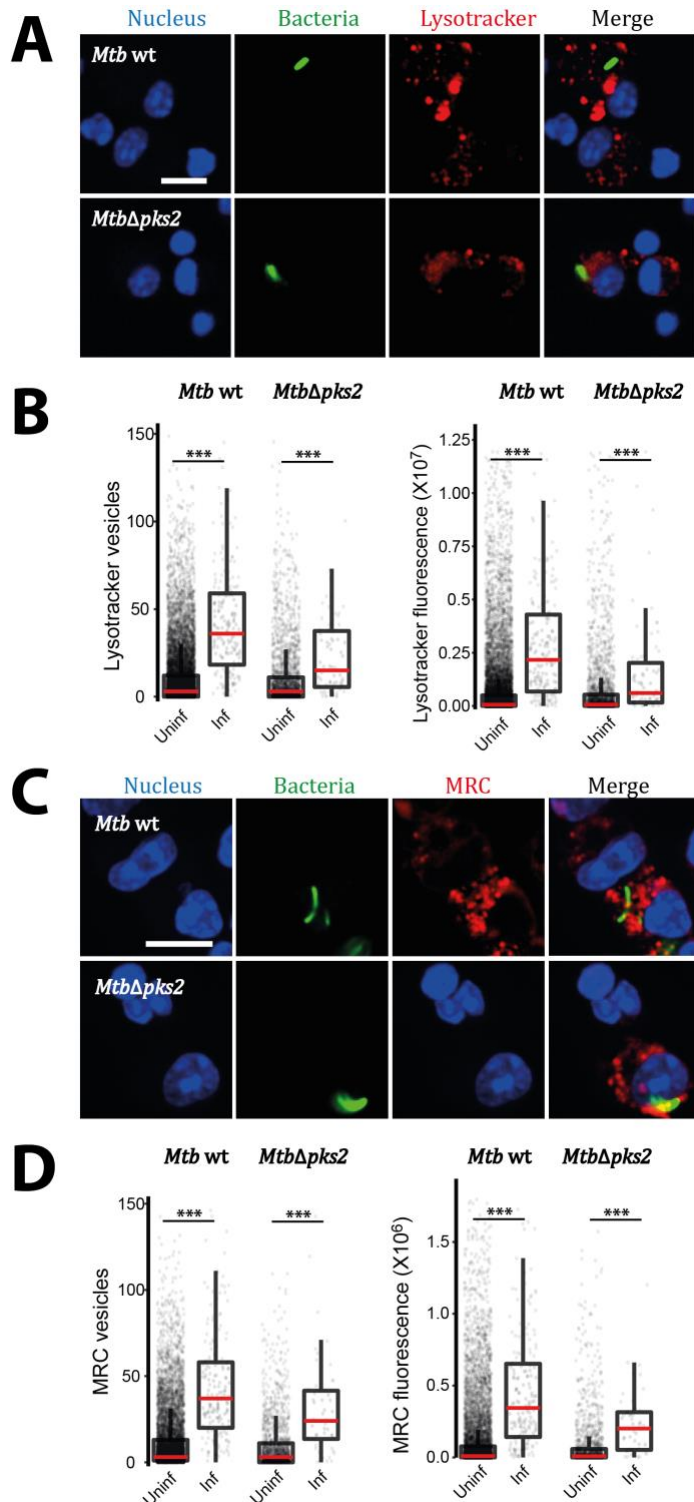
14

15

16

17

18



1

2

3 **FigS7. Wild type and *MtbΔpks2* infected cells show higher lysosomal content**

4 **compared to their respective uninfected controls.** (A-D) C57BL/6N] mice were infected

5 with *Mtb wt* or *MtbΔpks2*-GFP CDC1551 by aerosol inhalation. Eight weeks post-infection,

6 macrophages were isolated from infected lungs by making single-cell suspension and were

7 pulsed with lysosomal probes, namely lysotracker red (A, B), and magic red cathepsin (MRC)

1 (C, D). Representative images are shown in A and C. Graphs in B and D show the number and
2 intensity of lysosomes in respective probes were compared between *Mtb* wt or *Mtb* Δ *pks2*
3 CDC1551 infected and uninfected cells. Results are compiled from four wild type *Mtb* and
4 three *Mtb* Δ *pks2* infected mice. Statistical significance was assessed using Mann-Whitney
5 test, *** denotes p-value of less than 0.001. Scale bar is 10 μ m.

6
7
8